CERN 84–04
3 April 1984

ORGANISATION EUROPÉENNE POUR LA RECHERCHE NUCLÉAIRE
CERN EUROPEAN ORGANIZATION FOR NUCLEAR RESEARCH

INTRODUCTION TO TRANSFER LINES AND CIRCULAR MACHINES

P.J. Bryant

Lectures given in the
Academic Training Programme of CERN
1983–1984

GENEVA
1984

CERN - Service d'information scientifique - RD/630 - 2500 - avril 1984

ABSTRACT

This course was given in the 1983-84 Academic Training Programme. It is designed as an elementary introduction to both the theory and the hardware for transfer lines and circular machines. The course is limited to linear problems and treats the topics of single particle motion in the transverse and longitudinal planes, emittance ellipses, parameterisation, optical properties of some specific modules, stabilities in the transverse and longitudinal planes, field and gradient errors, and scattering in thin windows.

CONTENTS

COORDINATE SYSTEMS AND FREQUENTLY USED SYMBOLS

Local coordinates for lenses

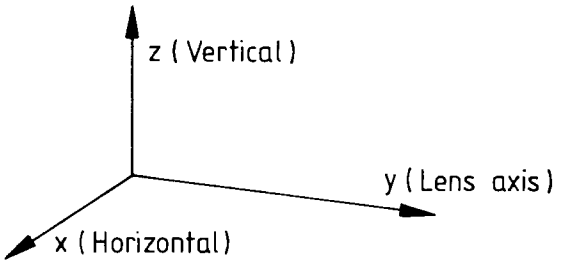

Local coordinates for cavities

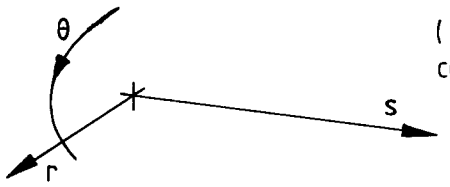

Local coordinates for the beam

y is used as general transverse coordinate for both x and z

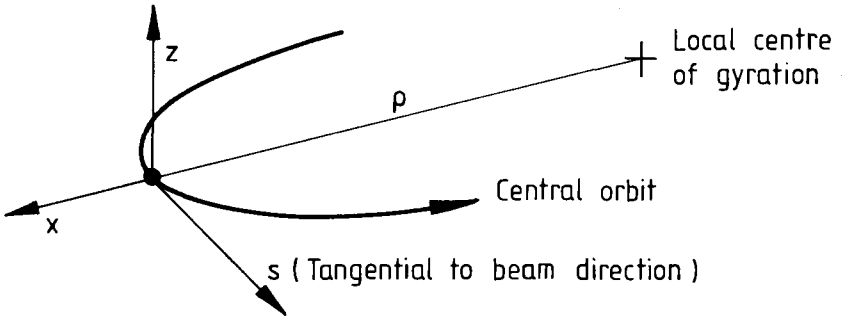

(MKS units)

R	average machine radius [m]
β_y	transverse betatron amplitude function [m] in plane (y,s)
α_y	$-\frac{1}{2}\frac{d\beta_y}{ds}$
γ_y	$(\frac{1+\alpha_y^2}{\beta_y})$ [m^{-1}]
μ_y	phase advance of betatron oscillation [rad]
Q_y	number of betatron oscillations per revolution in plane (y,s)
$\underline{P}$	particle momentum [GeV/c] ($\Delta p/p$ fractional momentum deviation)
D_y	transverse dispersion function [m] (local transverse co-ordinate of an off-momentum closed orbit normalised by $\Delta p/p$ - often denoted by α_p in the literature)
α	momentum compaction factor [m] (defined as $\Delta R/(\Delta p/p)$ but often defined as $(\Delta R/R)/(\Delta p/p)$ in the literature)
E_y	transverse emittance [π•m rad]
m	mass of ionised particle [kg]
e	charge of ionised particle [A s]
$\underline{v}$	particle velocity [m s^{-1}]
$\underline{F}$	force on ionised particle [N]
F,f	focal length of a lens [m]
$\emptyset$	magnetic scalar potential function [T m]
$\underline{B}$	magnetic flux density [T]
$\underline{H}$	magnetic field strength [Am^{-1}]
$\underline{E}$	electric field strength [Vm^{-1}] (the context should distinguish between emittance, E_y, and the component E_y of $\underline{E}$)
t	time [s]
ω_c	cyclotron frequency [rad s^{-1}]
ω_{rev}	revolution frequency of synchronous particle [rad s^{-1}]
$\omega_{r.f.}$	angular frequency of accelerating field [rad s^{-1}]
ϕ	phase of cavity voltage as ion traverses cavity [rad] (ϕ_s is phase for synchronous particle)
h	harmonic number ($\omega_s = h\omega_{r.f.}$)
γ	ratio of total energy of particle to its rest energy
γ_t	transition energy
β	v/c where c = velocity of light

The context should easily distinguish between these variables and γ_y and β_y even when the "y" subscript is dropped to shorten the formulae

E, E_s particle energy, synchronous particle energy [eV or J]

Ω synchrotron oscillation frequency [rad s^{-1}]

Y, Y' normalised variables used for transverse phase space

ϕ normalised betatron phase variable in a circular machine, $\phi(s) = \int_0^s \frac{ds}{Q\beta}$ [rad]

also used briefly in Section 2.1 as the scalar potential function for magnetic fields

' is frequently used to indicate differentiation. In normal space y' is dy/ds but in normalised space Y' is $dY/d\mu$

1. INTRODUCTION

All particle beams have a natural divergence and if left to propagate through free space they would spread out indefinitely. Such a situation may be acceptable over very short distances, but in most cases this growth in beam size must be stabilised by applying focusing forces. In the early cyclotrons (see Fig. 1 and Appendix A), this was done almost empirically by slightly diminishing the guiding magnetic field with orbit radius. As these machines evolved, a complete analysis was made of the focusing action and a simple criterion for focusing in the two transverse planes was obtained.

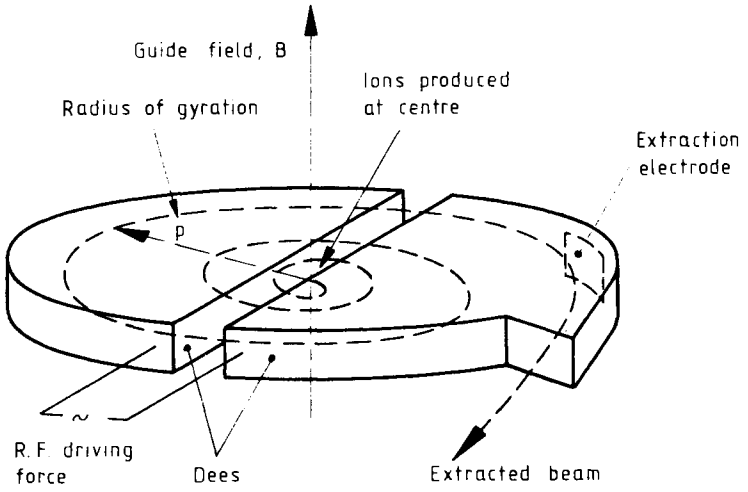

Fig. 1 Schematic cyclotron

Defining the Field Index,

$$n = - \frac{dB/B}{d\rho/\rho} ,$$

then for focusing in both transverse planes

$$0 < n < 1 \quad . \tag{1.1}$$

A complete family of machines (cyclotrons, synchro-cyclotrons, synchrotrons) based on this principle were developed. They are referred to as constant-gradient (CG) machines and also as weak focusing machines owing to the above limitation imposed on the field index.

In 1952 Courant, Livingston and Snyder proposed a more flexible way of focusing beams based on strong alternating field gradients. The idea had been suggested earlier by Christofilos but it was not published. This new principle is directly analogous to a well-known result in geometrical optics. The combined focal length, F, of a pair of lenses of focal lengths f_1 and f_2 separated by a distance, d, is given by

$$\frac{1}{F} = \frac{1}{f_1} + \frac{1}{f_2} - \frac{d}{f_1 f_2} .$$

If the lenses have equal and opposite focal lengths, $f_1 = -f_2$, this reduces to the simple form $F = f^2/d$ which is always positive. In fact, F remains positive over quite a large range of values when f_1 and f_2 have unequal values, but are still of opposite sign. It will be shown later, that quadrupole lenses focus charged particle beams in one plane while defocusing in the orthogonal plane. Thus a pair of opposed quadrupole lenses would have the optical equivalent of Fig. 2 and would be focusing in both planes.

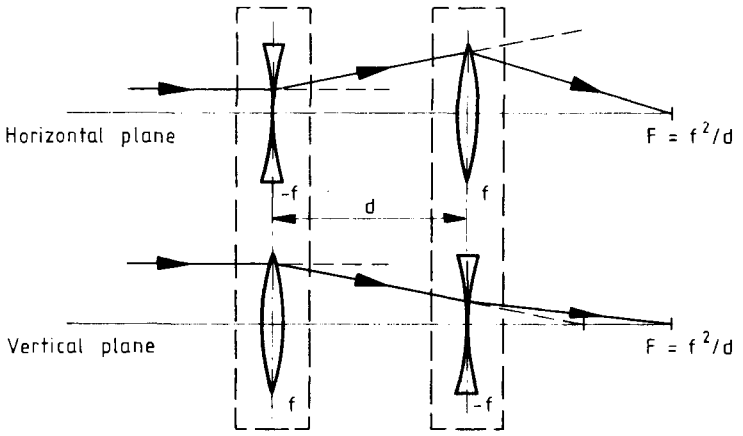

Fig. 2 Optical equivalent of a pair of opposed quadrupoles

Within certain limits a long series of alternating lenses will focus. Intuitively one sees that although the beam may be defocused by one lens, it arrives at the following lens further from the axis and hence is focused more strongly. Structures based on this principle are referred to as alternating gradient (AG) structures and because the field index is no longer restricted and can be conveniently made much greater than 1 to focus more strongly so as to reduce beam sizes, these structures are also referred to as strong focusing structures.

In these lectures, I shall confine myself to discussing mainly AG, strong-focusing structures, which are now used for all large accelerators and transfer lines, but in fact many of the characteristics of weak focusing structures will naturally appear in the theory as it is developed. As the lectures are designed as an introduction I will include descriptions of hardware, physical explanations and analogies where they appear useful.

2. MAGNETIC LENSES

AG structures in their basic form are built up from individual dipole and quadrupole lenses, which determine the structures' geometry and focusing, respectively. These two basic lenses determine what is known as the linear optics of the structure. In this chapter, higher order lenses will also be described as a simple and logical extension to the series, but in the subsequent chapters only linear optics problems will be dealt with as the non-linear behaviour of AG structures falls well beyond these lectures.

2.1 Multipole potentials for transverse field lenses

The ideal fields for an AG structure are purely transverse and can be expressed in the current-free aperture of the lens using a scalar potential function, $\emptyset$, in the form of a polynomial expanded about the lens' axis,

$$\emptyset = \emptyset_0 + \sum_1^\infty r^m \left[a_m \cos(m\theta) + b_m \sin(m\theta)\right], \tag{2.1}$$

where a_m and b_m are constant amplitude factors. m = integer.

The polar co-ordinate form above is general and can be used to express any transverse field. It is useful in lens design work and in lens measurement using rotating coils. The sine terms will be designated "right multipoles" and the cosine terms "skew multipoles". It will be shown later that the beam in an AG structure has two independent orthogonal, normal modes of oscillation and it will turn out that the choice of right lenses will make these modes horizontal and vertical. This in turn makes it more convenient to use Cartesian co-ordinates (see Fig. 3) for optics calculations.

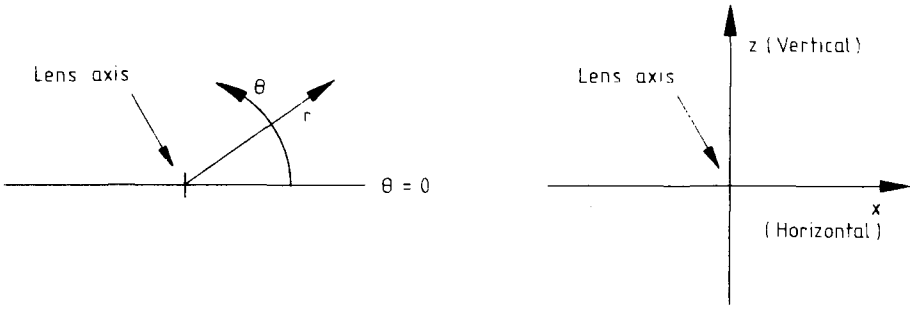

Fig. 3 Local co-ordinate systems for lenses

A quick way of transforming Eq. (2.1) into Cartesian co-ordinates is to use complex notation, defining skew lenses as real and right lenses as imaginary. Remembering that $[\cos(m\theta) + j \sin(m\theta)] = (\cos\theta + j \sin\theta)^m$ (De Moivre's Formula) we get:

$$\emptyset = \emptyset_0 + \sum_1^\infty a_m \, \mathrm{Re}\,(r\cos\theta + jr\sin\theta)^m + b_m \mathrm{Im}(r\cos\theta + jr\sin\theta)^m \tag{2.2}$$

$$\emptyset = \emptyset_0 + \sum_1^\infty a_m \, \mathrm{Re}\,(x + jz)^m + b_m \mathrm{Im}(x + jz)^m .$$

The field components are obtained by differentiation, e.g. $B_x = -\partial\emptyset/\partial x$, as given in Table 1.

Table 1

Potentials and Field Components in Multipole Lenses

Multipole	Right lenses $\emptyset_n = b_n \mathrm{Im}(x+jz)^n$	Skew lenses $\emptyset_n = a_n \mathrm{Re}(x+jz)^n$
Dipole+, n = 1	$\emptyset_1 = b_1 z$ $B_x = 0,\ B_z = -b_1$	$\emptyset_1 = a_1 x$ $B_x = -a_1,\ B_z = 0$
Quadrupole, n = 2	$\emptyset_2 = 2b_2 xz$ $B_x = -2b_2 z$ $B_z = -2b_2 x$	$\emptyset_2 = a_2(x^2-z^2)$ $B_x = -2a_2 x$ $B_z = 2a_2 z$
Sextupole, n = 3	$\emptyset_3 = b_3(3x^2z-z^3)$ $B_x = -6b_3 xz$ $B_z = 3b_3(z^2-x^2)$	$\emptyset_3 = a_3(x^3-3xz^2)$ $B_x = 3a_3(z^2-x^2)$ $B_z = 6a_3 xz$
Octupole, n = 4	$\emptyset_4 = 4b_4(x^3z-xz^3)$ $B_x = -12b_4 x^2z + 4b_4 z^3$ $B_z = -4b_4 x^3 + 12b_4 xz^2$	$\emptyset_4 = a_4(x^4+z^4-6z^2x^2)$ $B_x = -4a_4 x^3 + 12a_4 z^2 x$ $B_z = -4a_4 z^3 + 12a_4 x^2 z$
" " etc.	" " etc.	" " etc.

+ The horizontal field dipole naturally falls into the skew category, but it is never referred to as a skew lens.

It is clear from Eq. (2.1) that right* and skew lenses are physically identical but are mutually rotated by $\pi/2n$. The ideal pole profiles for exciting the various multipoles are simply equi-potential surfaces, but since in practice the pole has to be truncated, both transversely and axially it may be necessary to modify the shape to obtain the required field quality.

* In the later sections the word 'right' will be omitted in line with normal practice.

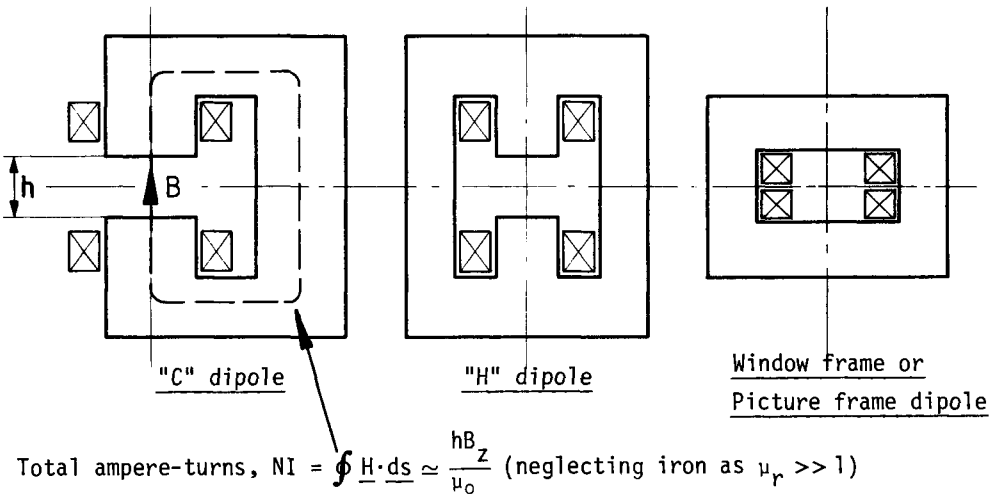

Total ampere-turns, $NI = \oint \underline{H} \cdot \underline{ds} \simeq \frac{hB_z}{\mu_o}$ (neglecting iron as $\mu_r >> 1$)

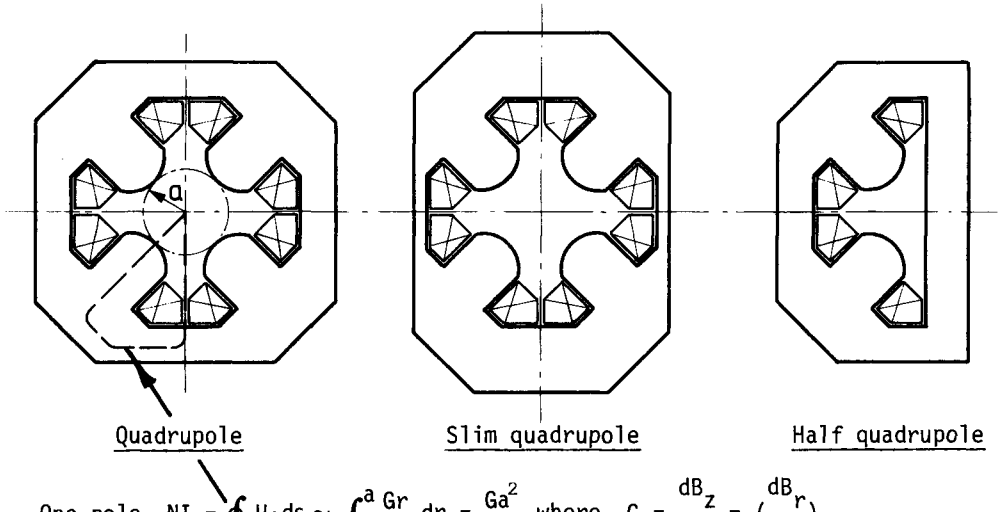

One pole, $NI = \oint \underline{H} \cdot \underline{ds} \simeq \int_0^a \frac{Gr}{\mu_o} dr = \frac{Ga^2}{2\mu_o}$ where, $G = \frac{dB_z}{dx} = \left(\frac{dB_r}{dr}\right)_{45^\circ}$

$= -2b_2$

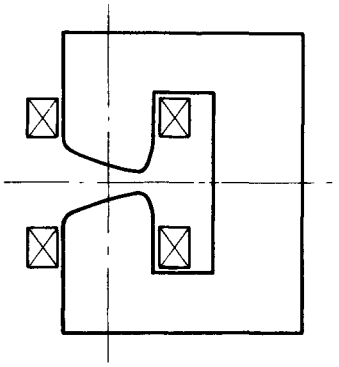

NI = number of ampere-turns [A]
h = dipole gap height [m]
a = inscribed circle radius [m]
s = integration path [m]
H = magnetic field strength [A m^{-1}]

Fig. 4 Practical lenses

2.2 Practical lenses

The schematic cross-sections of practical magnets of the dipole and quadrupole types are shown in Fig. 4 with the approximate expressions for the ampere turns needed to excite them.

The detailed design of such magnets is very complicated. The specified field quality usually requires the designer to compensate for the truncation of the pole in the transverse and axial directions and to take care of non-uniform saturation effects. To do this, the pole profile can be specially shaped both in the transverse and axial directions. Alternatively, or more usually to complement the profile correction, shims are added along the length of the pole or at the ends during the magnetic measurements.

Structures built up of pure dipoles and pure quadrupole lenses are called separated function structures. However, it is relatively easy to combine many multipoles in the same magnet and structures with magnets combining the dipole and quadrupole fields in a single unit are called combined function magnets. Typically these magnets are of the "C" design as shown in Fig. 4.

2.3 Hard edge approximation

In order to simplify the optics calculations, it is necessary to replace the real-world magnet by an idealised version, referred to as the hard edge model (see Fig. 5). In this model the integral of the field or multipole of interest through the magnet is replaced by the central value times an effective length.

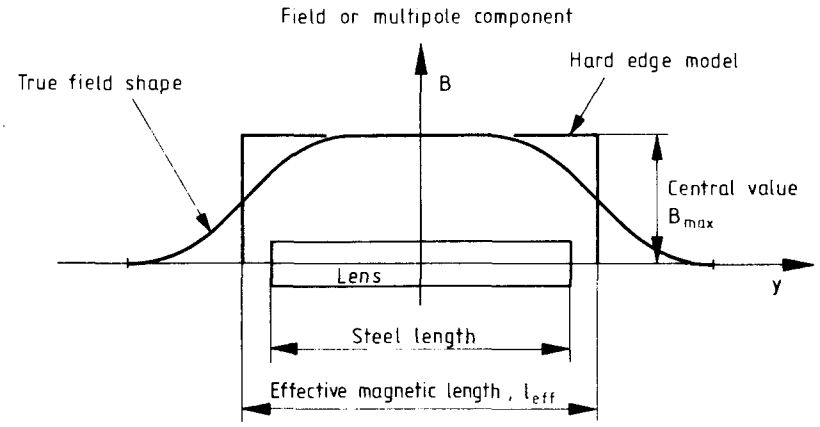

Fig. 5 Hard edge model

Clearly such a model neglects many things, but with some additional effort the true shape of the end field can be more closely approximated by having adjacent blocks of field of diminishing strength and several computer codes will allow the superposition of hard edge models, when more than one multipole must be considered as in combined function magnets, providing the same effective length is used. The longitudinal components in the end fields, however, are completely lost in this model. These components do enter into edge focusing and the hard edge model has to be modified slightly to include them (see section 3.5.2). They also excite non-linear coupling resonances but this is beyond the scope of the present lectures, but fortunately their effect is rarely of any importance.

In conventional magnets, the effective field lengths exceed the iron length but in superconducting magnets it is the contrary. Table 2 gives approximations for the effective field lengths and central fields in conventional lenses whose gaps or inscribed apertures are far less than the iron yoke length.

Table 2

Approximations for the effective field lengths and central fields of lenses in which the gaps or inscribed apertures are much less than the iron yoke length and the iron is unsaturated

Multipole	Effective magnetic length	Central field
Dipole	$\ell_{eff} \simeq \ell_{iron} + 1.3\ h\ \{0.7\ h\}$	$B_0 \simeq \frac{\mu_0 N_p I}{h/2}$
Quadrupole	$\ell_{eff} \simeq \ell_{iron} + a\ \{0.6\ a\}$	$G_0 \simeq \frac{2\mu_0 N_p I}{a^2}$
Sextupole	$\ell_{eff} \simeq \ell_{iron} + 0.5\ a$	$G'_0 \simeq \frac{6\mu_0 N_p I}{a^3}$

Notation

h = the dipole gap height [m]

a = radius of inscribed circle for multipole lenses [m]

ℓ_{iron} = yoke length [m]

Values in { } for the dipole and quadrupole indicate the reduced effective length when the iron is saturated

$N_p I$ are the required ampere turns per pole [A]

3. EQUATIONS OF MOTION

The purpose of an AG structure is to transmit a large number of particles over long distances and often through large angles, while keeping all of their trajectories grouped together, i.e. focused. This description of the action of the structure already suggests, that it would be reasonable to analyse the problem in two stages. Firstly one searches for an orbit, which satisfies the needs, and then one expresses similar orbits in the co-ordinate system of the first ideal orbit, in the hope of finding a set of orbits which behave as required.

3.1 Central orbit

Rather naïvely, the central orbit can be defined as the ideal trajectory through the transfer line or accelerator for particles of the design momentum.

In a separated function structure, this trajectory coincides with the axes of the quadrupoles. Since quadrupoles (as well as all higher order multipoles) have zero field on their axes, the geometry of the central orbit is then solely determined by the dipoles. Turning the problem round, one first positions the dipoles when designing a structure. This appears simple at first sight, but it will become clear later that the detailed positioning of the dipoles is important for particles whose momentum is slightly different to that of the central orbit.

In combined function structures, there is no clear reference such as the quadrupole axes in the previous case, and the central orbit is a more arbitrary choice and merits better the name ideal orbit.

In many practical cases, the central orbit may be somewhat difficult to determine. For example, transfer lines are often required to pass through the fringe fields of other structures and in colliders the beams are often influenced by the analysing magnets of the experiments. One solution is to create a field map and to track through that map. This is dealt with in Appendix B. Once this has been done the field can be expanded in a multipole series about the orbit, again by using the field plot. Knowing the distribution of the dipole and quadrupole fields, the designer is then in a position to continue and to calculate the linear optics of the whole structure.

3.2 Betatron oscillations

We start by considering a small volume of space through which the central orbit passes (see Fig. 6). The central orbit can be thought of as comprising segments of uniform cyclotron motion as described in Appendix A, even if these segments have to be made vanishingly small as in a combined function magnet or of infinite radius of curvature as in field-free regions. The only restrictions that we shall impose at this stage are that the field is everywhere perpendicular to the local segment of the central orbit and that $B_x = 0$ in the plane of the central orbit.

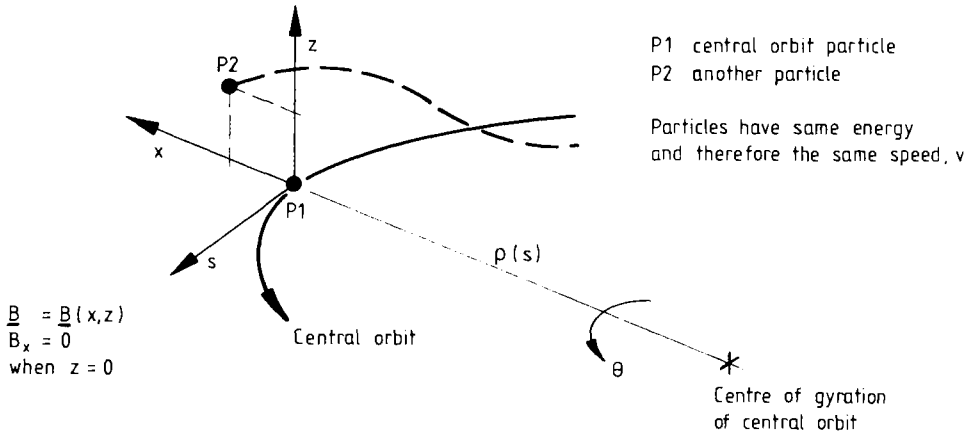

Fig. 6 Betatron oscillations

We now include one other particle, which has the same energy and speed but is on a nearby orbit. This particle will also have an associated radius of curvature and instantaneous centre of gyration, but we are more interested in expressing its motion with reference to the central orbit. For this we will use a new local system of co-ordinates (x,z,s), which has its origin on the central orbit. The x-axis is the prolongation of the radius of curvature of the central orbit and the z-axis is perpendicular to the plane of the local segment of the central orbit.

Considering each particle in turn, we can interpret its local segment of orbit as a cyclotron motion and we can equate the radial acceleration, evaluated using polar co-ordinates centred on the centre of gyration of the central orbit, to the magnetic deflection force. The general expression for radial acceleration is given by

$$A_r = \left[\frac{d^2\rho}{dt^2} - \rho\left(\frac{d\theta}{dt}\right)^2\right] .$$

For the central orbit $d^2\rho/dt^2$ is zero, but for the general orbit it must be included, since this orbit has a different centre of gyration. The second term $\rho(d\theta/dt)^2$ is more familiar as v^2/ρ.

$$\underline{\text{Central orbit}}: \quad m\frac{d^2\rho}{dt^2} \; (=0) \; - \frac{mv^2}{\rho} = eB_0 v \tag{3.1}$$

$\underline{\text{General orbit}}$:

$$\text{x-component:} \quad m\frac{d^2}{dt^2}\,(x+\rho) - \frac{mv^2}{(x+\rho)} = eB_z v \tag{3.2}$$

$$\text{z-component:} \quad m\frac{d^2z}{dt^2} = -eB_x v \tag{3.3}$$

We will now add one further restriction that $x \ll \rho$. This is otherwise known as imposing paraxial conditions. In fact it is easily satisfied, since transverse beam dimensions are typically measured in millimetres, whereas bending radii are usually tens of metres. Using this and the fact that ρ is constant, Eq. (3.2) can be reduced to

$$m \frac{d^2x}{dt^2} - \frac{mv^2}{\rho}\left(1 - \frac{x}{\rho}\right) = eB_z v \ . \tag{3.4}$$

As was described in Chapter 2, a 2-dimensional field can be expanded about an axis in terms of multipole fields. By doing this about the s-axis, we can relate B_x and B_z to B_0 on the central orbit. However, we have specified that $B_x = 0$ when $z = 0$, which excludes all skew multipoles and to keep the problem linear we limit the expansion to first order (quadrupole).

$$\begin{aligned} B_z &= B_0 + x \left.\frac{\partial B_z}{\partial x}\right|_0 = B_0 \left(1 - \frac{n}{\rho} x\right) \\ B_x &= z \left.\frac{\partial B_x}{\partial z}\right|_0 = -z \frac{B_0 n}{\rho} \ . \end{aligned} \tag{3.5}$$

Remembering that, $\partial B_x/\partial z = \partial B_z/\partial x$, since curl $\underline{B} = 0$ and the definition of n from Eq. (1.1).

By substituting Eq. (3.5) into (3.4) and (3.3) and using the expressions for the cyclotron motion from Appendix A Eq. (A5) $\omega_c = |B_0 e/m|$ and Eq. (A6) $B_0 e/m = -v/\rho$, we find the simple equations

$$\begin{aligned} \frac{d^2x}{dt^2} + \omega_c^2(1-n)x &= \frac{d^2x}{dt^2} + \frac{v^2}{\rho^2}(1-n)x = 0 \\ \frac{d^2z}{dt^2} + \omega_c^2 nz &= \frac{d^2z}{dt^2} + \frac{v^2}{\rho^2} nz = 0 \ . \end{aligned} \tag{3.6}$$

Equations (3.6) (formulation with ω_c) are the Kerst-Serber equations for betatron oscillations, which were first derived and applied for weak focusing machines. By inspection one can see that the solutions are stable oscillations if

$$\begin{aligned} n &< 1 \text{ in the x-s plane} \\ n &> 0 \text{ in the z-s plane.} \end{aligned}$$

Thus if we wish to satisfy both planes simultaneously:

$$0 < n < 1 \ . \tag{3.7}$$

Hence we have derived the weak focusing criterion for constant gradient machines mentioned in the introduction.

We should note at this stage that by excluding skew multipoles and right multipoles above quadrupole, the motions in the two planes are completeley decoupled and linear.

When considering strong focusing structures, where $|n|$ can be greater than unity, it is convenient to transform Eqs. (3.6) into a form familiar to AG specialists. Firstly the independent variable is changed from time, t, to distance along the central orbit, s, by simply applying ds = vdt and a new variable K(s) is defined such that

$$K(s) = \begin{cases} \left(\frac{1-n}{\rho^2}\right) = \left(\frac{1}{\rho^2} + \frac{1}{B\rho}\frac{dB_z}{dx}\right) & \text{x-s plane} \\ \\ \frac{n}{\rho^2} = -\frac{1}{B\rho}\frac{dB_z}{dx} & \text{z-s plane} \end{cases} \tag{3.8}$$

Equations (3.6) now simply become

$$\frac{d^2y}{ds^2} + K(s)y = 0 \quad , \tag{3.9}$$

where y is introduced as the general transverse variable, replacing both x and z.

It is clearly natural to assume the z-axis to be vertical, as circular machines are usually built in the horizontal plane, but nothing prevents us turning Fig. 6 through 90^0 and considering elements with vertical bending, in which case K_z would have the form

$$\left(\frac{1}{\rho^2} - \frac{1}{B\rho}\frac{dB_z}{dx}\right) .$$

This would in fact be essential for many transfer lines.

Although in the combined function field of Fig. 6 the x and z variants of K(s) look different, it turns out in practice that n is of the order of several hundred, thus (1-n) $\simeq$ -n and the two planes are virtually symmetric.

If the field is a pure quadrupole, there will be no bending and $\rho_0 \to \infty$ yielding

$$K_x = -K_z = +\frac{1}{B_0\rho}\frac{dB_z}{dx}$$

(note that $B_0\rho$ = 3.3356 p from Eq. (A8) and is constant even if we choose to send $\rho_0 \to \infty$ and $B_0 \to 0$).

If the field is a pure dipole field, then

$$\frac{dB_z}{dx} = \frac{dB_x}{dz} = 0$$

and

$$K_x = \frac{1}{\rho^2} , \quad K_z = 0 .$$

Thus there is some weak focusing due to a pure dipole field in the plane of bending. This is illustrated in Fig. 7 and is the basis of focusing in a 180^0 spectrometer.

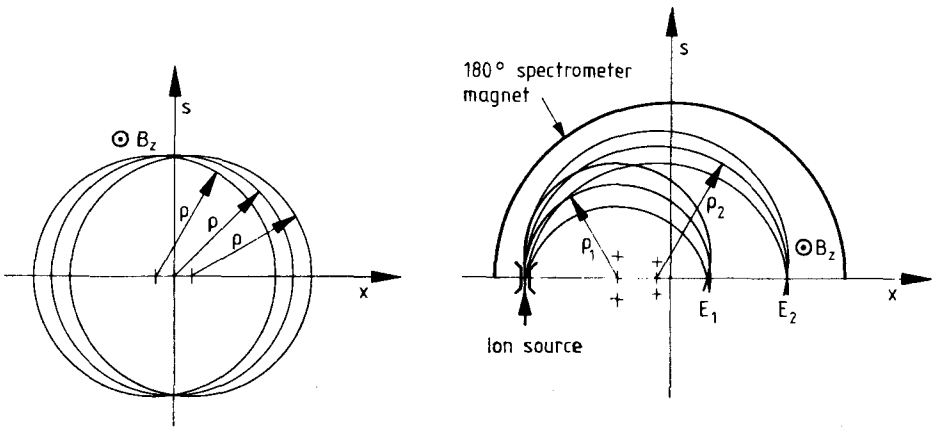

Fig. 7 Dipole zero-gradient focusing

We specified in Fig. 6 that $B_x = 0$ in the x-s plane. In fact, we could relax this condition and accept a tilted dipole field as shown in Fig. 8, in which case K(s) has the form $1/\rho^2$ in both planes with the appropriate ρ-values. It could also take the form $(1-n)/\rho^2$, but such lenses do not exist. It would not, for example be any good tilting a combined function dipole and quadrupole since this would introduce a skew gradient and couple the two planes.

Finally, if there is no field at all, i.e. a drift space, then

$$K(s) = 0 .$$

Table 3 summarises the various forms K(s) can assume.

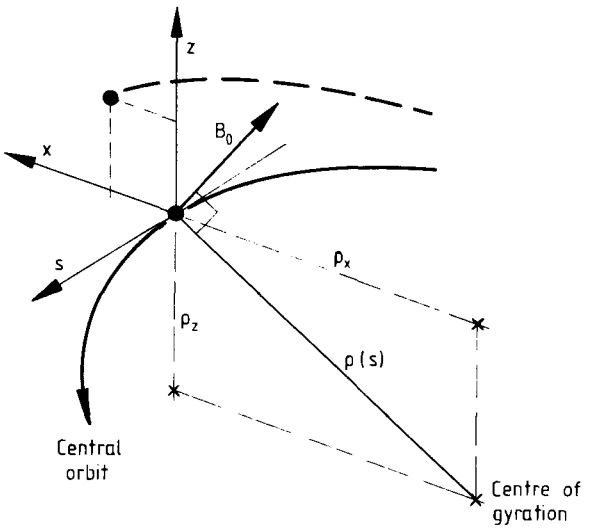

Fig. 8 Tilted dipole

Table 3

Forms for K(s)

Magnet	K_x	K_z
Combined function with vertical dipole field	$\frac{1}{\rho_x^2} + \frac{1}{B_0\rho}\frac{dB_z}{dx}$	$-\frac{1}{B_0\rho}\frac{dB_z}{dx}$
Combined function with horizontal dipole field	$\frac{1}{B_0\rho}\frac{dB_z}{dx}$	$\frac{1}{\rho_z^2} - \frac{1}{B_0\rho}\frac{dB_z}{dx}$
Quadrupole	$\frac{1}{B_0\rho}\frac{dB_z}{dx}$	$-\frac{1}{B_0\rho}\frac{dB_z}{dx}$
Vertical dipole field	$1/\rho_x^2$	0
Horizontal dipole field	0	$1/\rho_z^2$
Tilted dipole field	$1/\rho_x^2$	$1/\rho_z^2$
Drift space	0	0

The solution of Eq. (3.9) depends on the form of K(s), which in an AG structure is a step-like function, but of course, it is in principle easy to make a step-like solution by solving each region of constant K(s) independently and then combining the solutions. It is convenient to use a matrix form and eliminate the constants of integration using the initial conditions at the entry to the step.

Thus we find

$$K > 0 \text{ Focusing} \quad \begin{pmatrix} y \\ y' \end{pmatrix}_2 = \begin{pmatrix} \cos\phi & \frac{1}{\sqrt{K}}\sin\phi \\ -\sqrt{K}\sin\phi & \cos\phi \end{pmatrix} \begin{pmatrix} y \\ y' \end{pmatrix}_1 \tag{3.10}$$

$$K < 0 \text{ Defocusing} \quad \begin{pmatrix} y \\ y' \end{pmatrix}_2 = \begin{pmatrix} \cosh\phi & \frac{1}{\sqrt{-K}}\sinh\phi \\ \sqrt{-K}\sinh\phi & \cosh\phi \end{pmatrix} \begin{pmatrix} y \\ y' \end{pmatrix}_1 \tag{3.11}$$

$$K = 0 \text{ Defocusing} \quad \begin{pmatrix} y \\ y' \end{pmatrix}_2 = \begin{pmatrix} 1 & \ell \\ 0 & 1 \end{pmatrix} \begin{pmatrix} y \\ y' \end{pmatrix}_1 \tag{3.12}$$

where ℓ is the length of element = $(s_2 - s_1)$, y' is the longitudinal derivative dy/ds and $\phi = \sqrt{|K|}\,\ell$.

From Table 3 and Eqs. (3.10) to (3.12), we can see that quadrupoles focus in one plane, while defocusing in the other. Usage specifies that if a quadrupole focuses in the horizontal plane, it is called a focusing quadrupole (see Fig. 9).

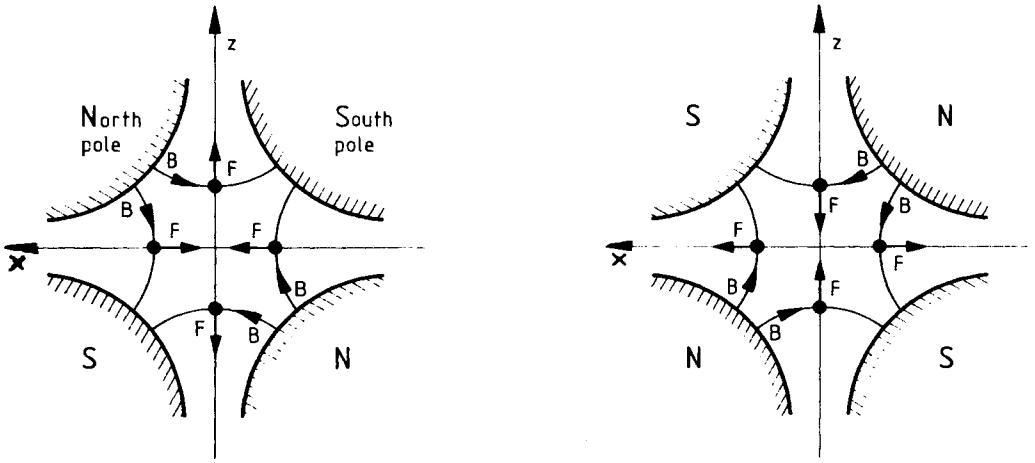

Focusing-F type Defocusing-D type

Fig. 9 Fields and forces inside a quadrupole
(Drawn for positively charged particles leaving the paper)

If we represent the matrix of the i^{th} element in a structure by M_i, then the solution for transmission through the whole structure would be

$$M = M_n \ldots M_{i+1} M_i \ldots M_1 \ . \tag{3.13}$$

The trajectory through the elements of the structure would be a continuous set of hyperbolic, sinusoidal and linear segments and it is clear that a series of elements could be chosen with alternating K-values separated by drift spaces such that the motion would be quasi-oscillatory and remain well-focused about the central orbit. Although this motion would not be smooth and periodic as in the weak focusing case, it is still referred to as a betatron oscillation.

The rather disjointed appearance of the real-space motion would be due to the loss of continuity in the second derivative of the amplitude at boundaries between elements, where the function K(s) changes discontinuously, and to the arbitrary layout of the elements, which in the general case could not give K(s) a periodic form. Of course, the use of the matrix formalism does not exclude dividing a region of constant K into separate sections, so that the trajectory can be determined at as many points as is required. Whether this motion can be made stable in a circular structure is a problem left until Chapter 4. The use of matrices is particularly well-suited to such piecewise structures, but it can of course also be applied to constant gradient machines such as the cyclotron.

3.3 Thin lens approximation

The matrix equatons (3.10) and (3.11) for transmission through focusing and defocusing elements can be considerably simplified if the argument $\phi = \ell\sqrt{K}$ is much less than unity. The lens can then be replaced by an infinitely thin lens of strength $K\ell$ placed at the centre of the original lens

$$\begin{pmatrix} y \\ y' \end{pmatrix}_2 = \begin{pmatrix} 1 & 0 \\ \mp|K\ell| & 1 \end{pmatrix} \begin{pmatrix} y \\ y' \end{pmatrix}_1 \tag{3.14}$$

where

$$|K\ell| = \frac{1}{|F|} = \left| \frac{\ell}{B_0\rho} \frac{dB_z}{dx} \right| \tag{3.15}$$

The new variable, F, is recognisable as the focal length (see Fig. 10). The minus sign denotes focusing and the positive sign defocusing.

The simplifications of replacing sin ϕ and sinh ϕ by ϕ and cos ϕ and cosh ϕ by unity are well known and the accuracy is evident. It is less evident why ℓ has to be replaced by zero in the top right position of the matrix. In fact we require $\ell = 0$ so that the determinant of the matrix remains unity. All matrices must satisfy this requirement unless there is some special mechanism such as energy loss by radiation. The unit

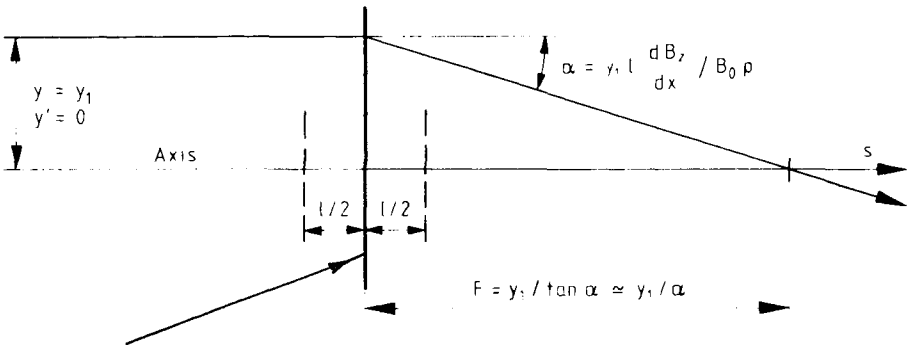

Thin lens (strength Kℓ, length zero) put at centre of the true lens of length ℓ.

Fig. 10 Focal length of a thin lens

determinant is an expression of Liouville's Theorem on the conservation of phase space volume. In the case of multi-dimensional matrices, there is a stronger requirement called the symplectic condition, which in the one-dimensional case becomes equivalent to Liouville's Theorem and the unit determinant.

The true length of the lens reappears of course in the drift spaces on either side. This approximation is good if the length of the original lens is much smaller than its focal length.

In separated-function, strong-focusing structures the $1/\rho^2$ focusing term in the dipoles is usually neglected on the grounds of it being small, although in accelerators most of the circumference is filled by dipole field.

Having made these approximations, transfer lines and circular machines are described by two simple matrices,

$$\begin{pmatrix} 1 & 0 \\ \mp\frac{1}{F} & 1 \end{pmatrix} \ldots \text{Eq. (3.14)} \quad \text{and} \quad \begin{pmatrix} 1 & \ell \\ 0 & 1 \end{pmatrix} \ldots \text{Eq. (3.12)}$$

In fact as machines progress towards TeV energies, these approximations improve and in this small way at least these big machines are simpler. The LEP lattice cell, for example, is more than adequately represented in this way with an accuracy better than 1% in the results.

3.4 Motion with a momentum deviation

So far we have derived equations for the motions of ions with small angle and position deviations from the central orbit, but beams are never mono-energetic, so we must also find equations for the motion of ions with a small momentum deviation.

We proceed as before by considering Fig. 6 and re-writing Eqs. (3.2) and (3.3) with an increase, dm, in the ion's mass and an increase, dv, in the ion's velocity. These increments are of course constant for any given particle.

$$(m + dm)\frac{d^2}{dt^2}(x + \rho) - \frac{(m+dm)(v+dv)^2}{(x+\rho)} = eB_z(v+dv) \tag{3.16}$$

$$(m + dm)\frac{d^2z}{dt^2} = -eB_x(v+dv) \ . \tag{3.17}$$

We start by making the same assumption as before that $x \ll \rho$ and in addition, that $dm \ll m$ and $dv \ll v$. By expanding and re-arranging the terms, we can obtain exactly the same equations as before with some new terms on the right-hand side.

$$\frac{d^2x}{dt^2} + \frac{v^2}{\rho^2}(1-n)x = -\frac{v}{\rho}\left(1 - \frac{n}{\rho}x\right)\left(-v\frac{dm}{m} + dv - \frac{dvdm}{m}\right) + \frac{2vdv}{\rho}\left(1 - \frac{x}{\rho}\right) + \frac{(dv)^2}{\rho}\left(1 - \frac{x}{\rho}\right)$$

$$\frac{d^2z}{dt^2} + \frac{v^2}{\rho^2}nz = \frac{nv^2z}{\rho}\left(\frac{dm}{m} - \frac{dv}{v} + \frac{dvdm}{mv}\right) \ .$$

Neglecting all second order terms in the small quantities, dv, dm, x, and z and changing the independent variable from t to s, gives

$$\frac{d^2x}{ds^2} + \frac{(1-n)}{\rho^2}x = \frac{1}{\rho}\left(\frac{dm}{m} + \frac{dv}{v}\right) = \frac{1}{\rho}\frac{dp}{p} \tag{3.18}$$

$$\frac{d^2z}{ds^2} + \frac{n}{\rho^2}z = 0 \quad , \tag{3.19}$$

using $\frac{dp}{p} = \left(\frac{dm}{m} + \frac{dv}{v}\right)$, where p is the momentum of the ion.

The z-s plane is then unchanged to the first order and is neglected here, while the x-s plane is modified by a constant term on the right-hand side. In fact, we are neglecting the source of chromaticity problems, but as this is an introductory course we have the right to do so.

The coefficient $[(1-n)/\rho^2]$ can be $1/\rho^2$ for a pure dipole or n/ρ^2 for a pure quadrupole, so we use K(s) as the general coefficient and we remember its various forms tabulated in Table 3. Thus we finally have the equation below, which is complementary to the betatron motion Eq. (3.9),

$$\frac{d^2y}{ds^2} + K(s)y = \frac{1}{\rho}\frac{\Delta p}{p} \quad , \tag{3.20}$$

where 'y' indicates the plane in which bending occurs whether it is x, z or both.

The solution to Eq. (3.20) is of the form

$$y = A \cos(\sqrt{K}\, s) + B \sin(\sqrt{K}\, s) + \frac{1}{\rho}\frac{\Delta p}{p}\frac{1}{K} .$$

As before, we create the complete solution by assembling piecewise the solution for each region of constant K(s). Using the entry conditions to each section the constants are found to be

$$A = \left(y_1 - \frac{1}{\rho}\frac{\Delta p}{p}\frac{1}{K}\right) , \quad B = y_1'/\sqrt{K} .$$

If we treat $\Delta p/p$ as a variable the result can be put into a 3 × 3 matrix form:

$K > 0$ Focusing

$$\begin{pmatrix} y \\ y' \\ \frac{\Delta p}{p} \end{pmatrix}_2 = \begin{pmatrix} \cos\phi & \frac{1}{\sqrt{K}}\sin\phi & \frac{1-\cos\phi}{\rho K} \\ -\sqrt{K}\sin\phi & \cos\phi & \frac{\sin\phi}{\rho\sqrt{K}} \\ 0 & 0 & 1 \end{pmatrix} \begin{pmatrix} y \\ y' \\ \frac{\Delta p}{p} \end{pmatrix}_1 \tag{3.21}$$

$K < 0$ Defocusing

$$\begin{pmatrix} y \\ y' \\ \frac{\Delta p}{p} \end{pmatrix}_2 = \begin{pmatrix} \cosh\phi & \frac{1}{\sqrt{-K}}\sinh\phi & \frac{\cosh\phi - 1}{-\rho K} \\ \sqrt{-K}\sinh\phi & \cosh\phi & \frac{\sinh\phi}{\rho\sqrt{-K}} \\ 0 & 0 & 1 \end{pmatrix} \begin{pmatrix} y \\ y' \\ \frac{\Delta p}{p} \end{pmatrix}_1 \tag{3.22}$$

The orbit of an off-momentum particle is usually expressed using a momentum dispersion function, D(s), such that

$$y = \frac{\Delta p}{p} D(s) \tag{3.23}$$

3.5 Edge focusing

So far we have considered regions of uniform K(s), or rather different magnetic elements, without worrying about the boundaries between them, except to define the hard edge model in Section 2.3. In some small weak focusing machines and in zero gradient synchrotrons a boundary effect called edge focusing is very important. A brief account of edge focusing is given here, although it is of less importance for AG structures and of virtually no interest in very large machines such as LEP.

If the boundary between elements is perpendicular to the central orbit, as is normally the case for quadrupoles, there is no edge focusing. The bending in dipoles first introduced edge focusing problems and then it was soon found to be convenient to intentionally slope the edges of dipoles to give focusing in early machines.

The focusing action arises in two ways.

3.5.1 Edge focusing in the plane of bending

In Fig. 11 two adjacent parallel ions having the same momentum are crossing a dipole.

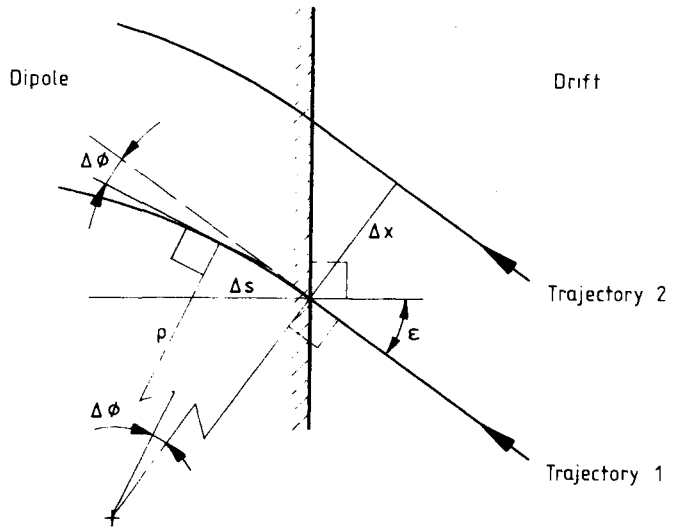

Fig. 11 Beam crossing the edge of a dipole at an angle ε to the normal

By the time the second ion reaches the magnet's edge, the first ion has already suffered a kick $\Delta\emptyset$, which is defocusing in the case of Fig. 11.

$$\Delta\emptyset = \frac{\Delta s}{\rho} = \frac{\Delta x}{\rho} \tan \varepsilon \ .$$

Thus the focal length of this edge lens is

$$F = \frac{\Delta x}{\Delta\emptyset} = \frac{\rho}{\tan \varepsilon} \ . \qquad (3.24)$$

This edge effect is very local and rather weak, so we can use the thin lens approximation of Section 3.3, Eq. (3.14):

$$\begin{pmatrix} y \\ y' \end{pmatrix}_2 = \begin{pmatrix} 1 & 0 \\ \frac{\tan \varepsilon}{\rho} & 1 \end{pmatrix} \begin{pmatrix} y \\ y' \end{pmatrix}_1 . \tag{3.25}$$

Figure 12 summarises the effects of slanting the dipole ends and the sign convention for ε.

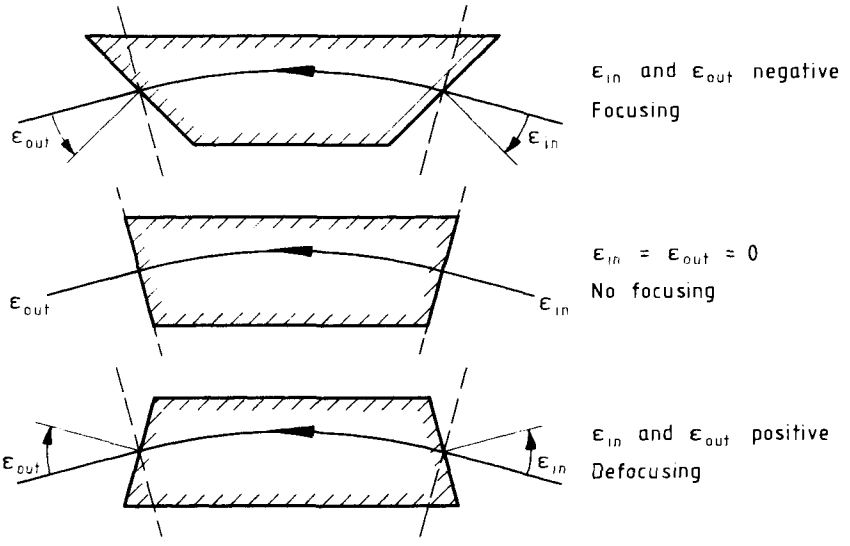

Fig. 12 Edge focusing in dipole in plane of bending

In the special case for which $\varepsilon_{in} = \varepsilon_{out} = 0$, the dipole is referred to as a sector magnet. For the standard parallel ended dipole ε is half the bending angle. The final magnet matrices are found by multiplying the central field matrix and the ends in the appropriate order.

3.5.2 Edge focusing perpendicular to the plane of bending

This effect invokes the action of the longitudinal field components in the fringe fields at the magnet ends. Figure 13 illustrates how these fields affect the focusing.

As in the earlier cases, by inclining the ends of the magnet the B_x component can be changed in sign and magnitude. The exact form of the fringe field may not be known and one is faced with a number of possibilities.

I am going to content myself here with just quoting a result assuming a linear drop-off of the fringe field.

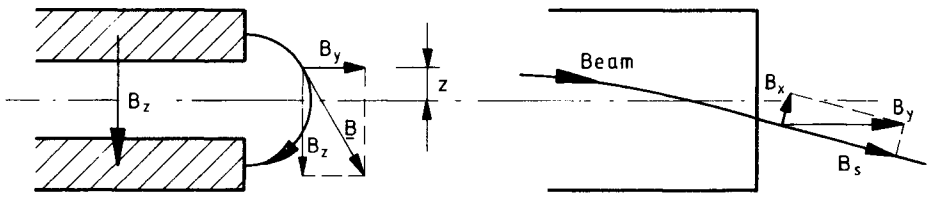

(assuming fringe field is purely 2-dimensional in y-z plane in the region of the beam)

Fig. 13 Focusing of longitudinal fringe fields in dipoles

$$\begin{pmatrix} y \\ y' \end{pmatrix}_2 = \begin{pmatrix} 1 & 0 \\ \frac{1}{\rho}\left(\frac{b}{6\rho\cos\varepsilon} - \tan\varepsilon\right) & 1 \end{pmatrix} \begin{pmatrix} y \\ y' \end{pmatrix}_1 \tag{3.26}$$

where b is the distance over which the fringe field drops linearly to zero.

4. MORE ABOUT BETATRON OSCILLATIONS

We have found that it is possible to build up a stepwise solution for an AG structure by solving each section and then multiplying the matrices together in the appropriate order. This appears to be a little disjointed* and lacking the beauty of smooth analytic functions, although it is perfectly valid. In a circular structure, there is of course an overall periodicity and by the nature of an AG structure the ions oscillate about the central orbit in a pseudo-harmonic manner. Would it be possible to extend this pseudo-harmonic behaviour and to choose a rather strange set of parameters for a given structure and to end up with the satisfaction of having simple harmonic motion for the solution?

4.1 Parameterisation

We start by writing a general solution for Eq. (3.9) given below:

$$\frac{d^2y}{ds^2} + K(s)y = 0 \tag{3.9}$$

$$y(s) = A\xi(s)\cos\left[\mu(s)+B\right] \quad , \tag{4.1}$$

where $\xi(s)$ and $\mu(s)$ are specially chosen and take into account the variation in the structure which is expressed in K(s). A and B are constants.

* The displacement and its first derivative are continuous and only its second derivative is discontinuous.

More specifically we define

$$\mu(s) = \int_0^s \frac{ds}{\xi^2(s)} \,. \tag{4.2}$$

By substituting Eq. (4.1) in (3.9) and using (4.2) in the differential form, $d\mu/ds = 1/\xi^2$ we find that $\xi(s)$ must satisfy the equation

$$\frac{d^2\xi}{ds^2} + K(s)\xi = \frac{1}{\xi^3} \,. \tag{4.3}$$

Traditionally, $\xi(s)$ is written as $\sqrt{\beta}(s)$ and the earlier equations become

$$y(s) = A\sqrt{\beta}(s) \cos [\mu(s) + B] \tag{4.4}$$

$$\mu(s) = \int_0^s \frac{ds}{\beta(s)} \,. \tag{4.5}$$

The function $\beta(s)$ is known as the betatron amplitude function and $\mu(s)$ as the betatron phase. Since we know $K(s)$, $\beta(s)$ and $\mu(s)$ can be determined. Finally, if we define $Y(s) = y(s)/\sqrt{\beta}(s)$, we have simple harmonic motion defined with the so-called normalised amplitude:

$$Y(s) = A \cos [\mu(s) + B] \,.$$

The function $K(s)$ can be retrieved at any point in the structure simply by combining the betatron amplitude function and its second derivative according to Eq. (4.3). On the other hand $\beta(s)$ depends upon the whole structure, as does also $\mu(s)$ the phase of the betatron oscillation. Thus the ion travels round the machine in real space with a kind of distorted sine wave whose amplitude varies as $\sqrt{\beta}(s)$ and whose phase advances unevenly as $1/\sqrt{\beta}(s)$.

The determination of $\beta(s)$ for any structure of appreciable complexity must be carried out by a computer, but assuming this can be done, further study of the structure can be made using the analytic form of Eq. (4.4).

4.2 Generalised transfer matrix

First we rewrite Eq. (4.4) as

$$y(s) = C\sqrt{\beta} \cos \mu + D\sqrt{\beta} \sin \mu \,, \tag{4.6}$$

where C and D are constants.

The derivative of y is easily obtained if we remember that $d\mu/ds = 1/\beta$ from Eq. (4.5). For convenience, we also define a new variable

$$\alpha = -\frac{1}{2}\frac{d\beta}{ds}$$

$$y'(s) = -\frac{C}{\sqrt{\beta}}(\alpha \cos \mu + \sin \mu) + \frac{D}{\sqrt{\beta}}(\cos \mu - \alpha \sin \mu) \ . \tag{4.7}$$

The initial conditions can be used to replace the constants C and D:

$$C = \frac{y_1}{\sqrt{\beta_1}} \ ; \quad D = \left(y'_1\sqrt{\beta_1} + \frac{y_1\alpha_1}{\sqrt{\beta_1}}\right) . \tag{4.8}$$

Although, it is a little more complicated than before, by substituting the expressions for the constants in Eq. (4.8) into the two Eqs. (4.6) and (4.7) one can verify quite easily the generalised transfer matrix $M(s_2|s_1)$ of Eq. (4.9),

$$M(s_2|s_1) = \begin{pmatrix} \sqrt{\frac{\beta_2}{\beta_1}}(\cos \mu + \alpha_1 \sin \mu) & \sqrt{\beta_1\beta_2} \sin \mu \\ -\left[\frac{(1+\alpha_1\alpha_2) \sin \mu + (\alpha_2-\alpha_1) \cos \mu)}{\sqrt{\beta_1\beta_2}}\right. & \sqrt{\frac{\beta_1}{\beta_2}}(\cos \mu - \alpha_2 \sin \mu) \end{pmatrix} \tag{4.9}$$

where

$$\mu = \int_{s_1}^{s_2} \frac{1}{\beta(s)} ds \ .$$

This form of transfer matrix is completely general.

If now we consider a circular structure comprising a series of identical periods, the function K(s) will be periodic, i.e. K(s) = K(s+L) where L is the period length. If K(s) is periodic the transfer matrix elements must also be periodic and by symmetry $\beta_1 = \beta_2 = \beta$ and $\alpha_1 = \alpha_2 = \alpha$. Thus for one period in a circular machine Eq. (4.9) reduces to

$$M(s) = \begin{pmatrix} (\cos \mu + \alpha \sin \mu) & \beta \sin \mu \\ -\gamma \sin \mu & (\cos \mu - \alpha \sin \mu) \end{pmatrix} \tag{4.10}$$

where

s and μ are for one period

α, β and γ are the entry/exit values and

$$\gamma = (1 + \alpha^2)/\beta \ . \tag{4.11}$$

α, β and γ are sometimes called the Courant and Snyder parameters and sometimes the Twiss parameters.

By inspection, it can be seen that this form of the generalised matrix can be split into two parts such that

$$M(s) = I \cos \mu + J \sin \mu \ ,$$

where

$$I = \begin{pmatrix} 1 & 0 \\ 0 & 1 \end{pmatrix} \quad \text{and} \quad J = \begin{pmatrix} \alpha & \beta \\ -\gamma & -\alpha \end{pmatrix}$$

and it is easily verified that

$$J^2 = -I$$

The algebra of M(s) is clearly the same as that of a complex number and we can apply De Moivre's formula which says that $(\cos \theta + j \sin \theta)^m = (\cos m\theta + j \sin m\theta)$. Thus for transmission through m identical periods of structure, each period having a phase advance, μ, the matrix is

$$M^m = I \cos (m\mu) + J \sin (m\mu)$$

and

$$(M^m)^{-1} = I \cos (m\mu) - J \sin (m\mu) \ .$$

Finally writing the matrix in full for transmission through m periods of a circular machine we get

$$M^m = \begin{pmatrix} \cos (m\mu) + \alpha \sin (m\mu) & \beta \sin (m\mu) \\ -\left(\frac{1+\alpha^2}{\beta}\right) \sin (m\mu) & \cos (m\mu) - \alpha \sin (m\mu) \end{pmatrix} \qquad (4.12)$$

4.3 Stability in a circular machine

Considering first a single cell, with a transfer matrix M, we search for eigenvectors, i.e. a vector (y,y') which when multiplied into M is returned multiplied by a simple factor λ, the eigenvalue.

$$M\begin{pmatrix} y \\ y' \end{pmatrix} = \lambda \begin{pmatrix} y \\ y' \end{pmatrix} \ .$$

Multiplying out, we find

$$(M_{11} - \lambda)y + M_{12}y' = 0$$
$$M_{21}y + (M_{22} - \lambda)y' = 0 \ .$$

Firstly we can solve for λ, by eliminating y and y' by dividing the two equations.

$$\lambda^2 - (M_{11} + M_{22})\lambda + (M_{11}M_{22} - M_{12}M_{21}) = 0 \ .$$

Now, it is easily verified that all the transfer matrices used so far have unit determinants, so that

$$\lambda^2 - (M_{11} + M_{22})\lambda + 1 = 0 \ .$$

Hence, there are two roots and two eigenvectors:

$$\lambda_{a,b} = \frac{1}{2}\left[M_{11} + M_{12} \pm \sqrt{(M_{11} + M_{22})^2 - 4}\right] \ . \tag{4.13}$$

Let us choose, $\cos \mu = (M_{11} + M_{22})/2$ in the secure hope that μ turns out to be the betatron phase advance μ already defined in Eq. (4.5).

Then Eq. (4.13) can be re-expressed as

$$\lambda_{a,b} = \cos \mu \pm j \sin \mu = e^{\pm j\mu} \ . \tag{4.14}$$

We do not need to evaluate the eigenvectors explicitly, but we can say that all initial conditions can be expressed as a linear sum of these two vectors, so that for transmission through m periods of structure

$$M^m V = A\lambda_a^m V_a + B\lambda_b^m V_b \quad , \tag{4.15}$$

where

V is a general vector (y,y')

V_a and V_b are the eigenvectors

A and B are constants, such that $V = AV_a + BV_b$.

In order that the motion is stable in Eq. (4.15) the eigenvalues λ_a and λ_b must be complex constants of unit modulus or in other words μ must be real in Eq. (4.14) and

$$\frac{1}{2}(M_{11} + M_{22}) = \left|\frac{1}{2} \text{ Trace } M\right| < 1 \ . \tag{4.16}$$

This is the stability criterion for a circular machine and of course it has to be satisfied in both planes.

For a thin lens structure of alternate focusing and defocusing lenses with a constant lens separation L, we have

$$M_{1\text{period}} = \begin{pmatrix} 1 & L \\ 0 & 1 \end{pmatrix}\begin{pmatrix} 1 & 0 \\ \frac{1}{F} & 1 \end{pmatrix}\begin{pmatrix} 1 & L \\ 0 & 1 \end{pmatrix}\begin{pmatrix} 1 & 0 \\ -\frac{1}{F} & 1 \end{pmatrix}$$

$$= \begin{pmatrix} 1 - \frac{L}{F} - \left(\frac{L}{F}\right)^2 & 2L + \frac{L^2}{F} \\ -\frac{L}{F^2} & 1 + \frac{L}{F} \end{pmatrix}$$

$$\cos \mu = \frac{1}{2} \text{ Trace } M = 1 - \frac{1}{2}\left(\frac{L}{F}\right)^2 .$$

Thus, $F > L/2$ for stability.

4.4 Emittance, an invariant of the motion

Returning to the basic equation for the betatron motion, in the form of Eq. (4.4), we have

$$y = A\sqrt{\beta} \cos (\mu + B) \tag{4.4}$$

$$y' = -\frac{\alpha A}{\sqrt{\beta}} \cos (\mu + B) - \frac{A}{\sqrt{\beta}} \sin (\mu + B) , \tag{4.17}$$

where

A and B are constants set by initial conditions,

β, μ, y and y' are all functions of s, and

remembering $d\mu/ds = 1/\beta$ and $\alpha = -1/2\ d\beta/ds$.

The phase terms can be eliminated between these two Eqs. (4.4) and (4.17).

$$A \cos (\mu + B) = y/\sqrt{\beta}$$
$$A \sin (\mu + B) = -(y'\sqrt{\beta} + \alpha y/\sqrt{\beta}) .$$

Squaring and adding, we find an invariant of the motion,

$$A^2 (= \text{constant}) = \left[\frac{y^2}{\beta} + (y'\sqrt{\beta} + \alpha y/\sqrt{\beta})^2\right] .$$

This is in fact the equation of an ellipse in (y,y') space, or phase space as it is known. The constant A^2 is equal to the ellipse area divided by π. Re-arranging slightly, we get

$$E = A^2\pi = \pi(\gamma y^2 + 2\alpha y y' + \beta y'^2) . \tag{4.18}$$

The area is here denoted by E, which is called the particle emittance (as opposed to the beam emittance which will be defined later).

There is some possible confusion here, since E is often defined as the (area)/π rather than the area. To avoid such confusion, one can write for example, E = (10 π) mm.mrad, showing that the π is included, whereas E = 31.4 mm.mrad leaves the reader guessing if π is included or whether it is the alternative definition.

If we now have many particles distributed around the same phase space ellipse at the entry to a structure, they are all characterised by the area of the ellipse, E and the initial shape of the ellipse. As they subsequently pass through the structure, the ellipse will change in shape according to the β, α and γ values, but its area E, remains constant as demanded by Eq. (4.18). Certain simple geometric properties of an ellipse can be used to find such quantities as the maximum excursion, maximum divergence, etc. at any point in a structure knowing the emittance and the α, β and γ values along the structure. Figure 14 lists some of these characteristics.

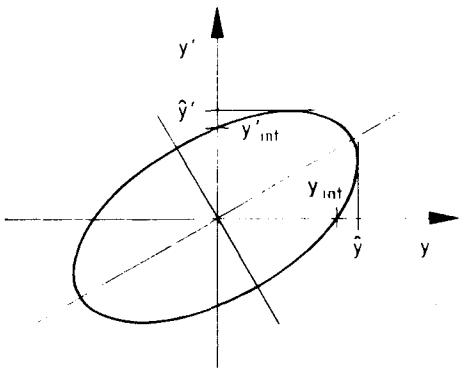

$$\hat{y} = \sqrt{\frac{E}{\pi}\beta}$$

$$\hat{y}' = -\alpha\sqrt{\frac{E}{\pi}\gamma}$$

$$y_{int} = \sqrt{\frac{E}{\pi\gamma}}$$

$$y'_{int} = \sqrt{\frac{E}{\pi\beta}}$$

Fig. 14 Geometric properties of an ellipse

In practice, we do not have single particles, or even small numbers of particles with the same invariant, E. Instead we have a beam comprising perhaps 10^{12}-10^{13} particles with most particles close to the central orbit and having small emittances and progressively fewer particles at larger emittances. In this case, we define a beam emittance, which is representative of the beam as a whole. Again there are possible confusions between the ways in which this is done. For these lectures, let us choose the definition which is used for measurements in the CERN machines. If the beam profile is measured, it is the population of the projected phase space ellipses which is seen (see Fig. 15). This population will normally be a near-Gaussian, but in fact this is not really that important. From the profile, the standard deviation of the distribution can be found, σ_y, and then we arbitrarily define the beam emittance as corresponding to a beam width of 2 σ_y.

$$E = \frac{(4\ \sigma_y^2)\pi}{\beta}, \quad \underline{\text{Beam emittance}}, \tag{4.19}$$

using the expression $\hat{y} = \sqrt{\frac{E}{\pi}\beta}$ and putting $\hat{y} = 2\ \sigma_y$.

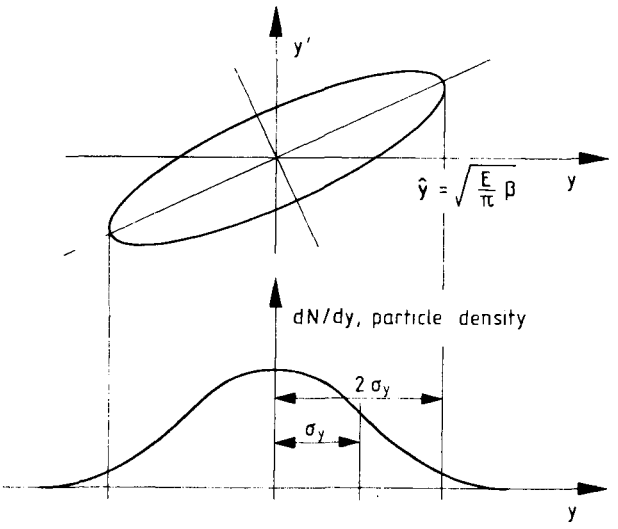

Fig. 15 Beam profile and its interpretation for emittance measurement

4.5 Distinctions between transfer lines and circular machines

Chapters 3 and 4 have been constructed so as to apply firstly to general structures and then to the special restricted cases of weak focusing and then AG circular machines. It is perhaps prudent, however, to think a little more about the distinctions between transfer lines and circular machines.

4.5.1 Circular machines

A circular structure has an imposed periodicity, which imposes the same periodicity on the Twiss parameters α, β and γ and in fact determines them uniquely. If one samples the co-ordinates of an ion after each successive turn in a circular machine, the points will fill out an ellipse given by Eq. (4.18). Only one set of α, β and γ values fit that ellipse. It is the periodicity of the structure which makes it possible for that specific ellipse to be returned unchanged turn after turn and for this reason it is called the matched ellipse. Now suppose one injects a beam of particles, which define a different ellipse (see Fig. 16). This ellipse is characterised by some other parameters, say α^*, β^* and γ^*, but the circular machine will not faithfully return this ellipse after each turn. Instead the ellipse will tumble round and round filling out a much larger ellipse of the matched ellipse form. It does not take long for the particles to filament and uniformly fill this matched ellipse.

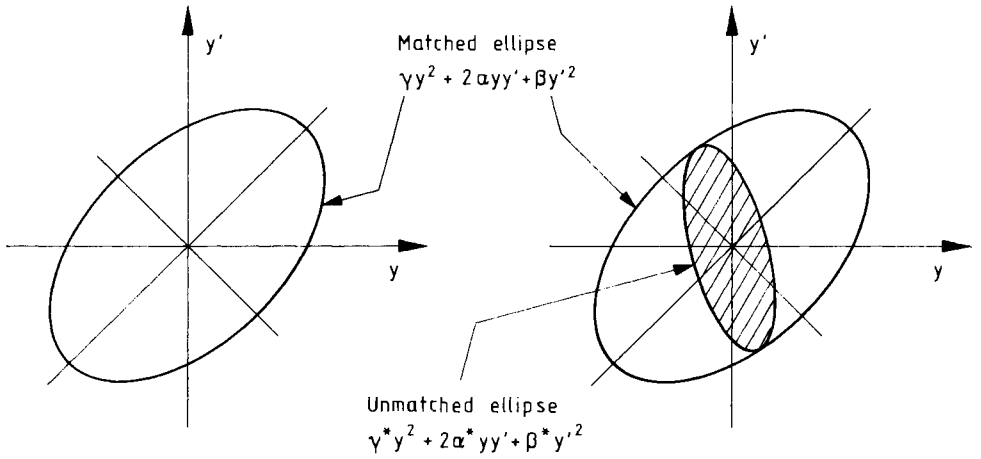

Fig. 16 Matched and unmatched ellipses

Since filamentation will quickly transpose any beam ellipse into the matched ellipse, there is no point in using and α, β and γ values other than the matched ones. Since α, β and γ depend on the whole structure any change at any point in the structure will in general (matched insertions excepted) change all the α, β and γ values everywhere.

4.5.2 Transfer lines

In a transfer line, there is no such restriction. The beam passes once and the shape of the ellipse at the entry to the line determines its shape at the exit. Exactly the same transfer line injected first with one emittance ellipse and then a different ellipse has to be accredited with different α, β and γ functions to describe the two cases. Thus α, β and γ depend on the input beam as well as the structure. Any change in the structure will only change the α, β and γ values downstream of that point.

4.6 Matched single-cell characteristics

The very large AG machines often have a basic lattice cell of the form shown in Fig. 17 and the parameters are such that the thin lens formula in Eq. (3.14) can be safely applied. By dividing up the cell as shown in Fig. 17 the maximum and minimum betatron amplitudes for the matched ellipse can be found.

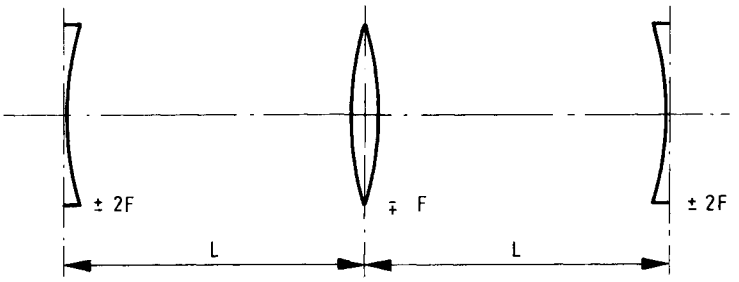

Fig. 17 Basic FODO cell

$$M = \begin{pmatrix} 1 & 0 \\ \frac{1}{2F} & 1 \end{pmatrix}\begin{pmatrix} 1 & L \\ 0 & 1 \end{pmatrix}\begin{pmatrix} 1 & 0 \\ -\frac{1}{F} & 1 \end{pmatrix}\begin{pmatrix} 1 & L \\ 0 & 1 \end{pmatrix}\begin{pmatrix} 1 & 0 \\ \frac{1}{2F} & 1 \end{pmatrix}$$

$$M = \begin{pmatrix} 1 - \frac{L^2}{2F^2} & 2L(1 - \frac{L}{F}) \\ -\frac{L}{2F^2}(1 + \frac{L}{2F}) & 1 - \frac{L^2}{2F^2} \end{pmatrix} \tag{4.20}$$

This matrix must be equivalent to the matched cell matrix in Eq. (4.10)

$$M = \begin{pmatrix} \cos\mu + \alpha \sin\mu & \beta \sin\mu \\ -(\frac{1+\alpha^2}{\beta}) \sin\mu & \cos\mu - \alpha \sin\mu \end{pmatrix}. \tag{4.10}$$

Since we have chosen the entry and exit points at symmetry planes, β must be a maximum or minimum and α is therefore zero, and

$$M = \begin{pmatrix} \cos\mu & \beta \sin\mu \\ -\frac{\sin\mu}{\beta} & \cos\mu \end{pmatrix}.$$

By inspection we see that

$$\cos\mu = (1 - 2\sin^2 \mu/2) \equiv (1 - \frac{L^2}{2F^2})$$

and

$$\sin\frac{\mu}{2} \equiv \pm\frac{L}{2F}.$$

Using the above, the strength of the lenses and the extrema of the betatron amplitude function can be simply expressed in terms of the cell half length, L, and phase advance, μ:

$$\text{lens strength} = \frac{1}{F} = \frac{2}{L}\sin\frac{\mu}{2} \tag{4.21}$$

$$\text{betatron extrema } \overset{\wedge v}{\beta} = \frac{2L}{\sin\mu}(1 \pm \sin\frac{\mu}{2}), \tag{4.22}$$

where

L is the half cell length

μ is the phase advance in the cell

5. ERRORS IN FIELD AND GRADIENT

In transfer lines there are two levels at which field and gradient changes are important. Firstly there are large changes for steering and optimisation. In this case, one uses the transfer matrices to predict the effect due to a field or gradient change. For example, to steer a beam onto a target, it is sensible to use a dipole placed upstream of the target such that there is a quarter betatron oscillation between them in order to get the best sensitivity. Likewise to control both position and angle two dipole correctors are needed again separated by a quarter wavelength. It is then simple matrix multiplication to find the effect of these two dipoles at a target or position monitor. The second level is for small changes, such as power supply ripple, misalignments and re-setting errors, which cause a mismatch at the end of the transfer line where the beam must arrive with the correct matched ellipse and central orbit to circulate in the accelerator. This problem is analysed in Section 5.1.

Once in the circular accelerator field errors or corrections to the orbit are dominated by the machine periodicity and are dealt with in Section 5.2. Power supply ripple will not be a problem in the same way as in the transfer line since its action will be adiabatic and the whole beam moves while conserving its emittance. Ripple is still a problem but beyond the present lectures. Finally whenever we talk about circular machines we are using the matched ellipse α, β and γ values although we are often rather slack about defining this.

5.1 Dipole and misalignment errors in transfer lines

The motion of a particle in a transfer line can be written as

$$y = A\sqrt{\beta}\,\sin(\mu + B) \tag{5.1}$$

[from rearranging Eq. (4.4)].

This motion is an ellipse in phase space with

$$y' = \frac{A}{\sqrt{\beta}}\cos(\mu + B) - \frac{A\alpha}{\sqrt{\beta}}\sin(\mu + B)\ . \tag{5.2}$$

Rearranging we have

$$\begin{aligned} Y &= y/\sqrt{\beta} = A\sin(\mu + B) \\ Y' &= y\alpha/\sqrt{\beta} + y'\sqrt{\beta} = A\cos(\mu + B), \end{aligned} \tag{5.3}$$

where (Y,Y') are known as normalised phase space co-ordinates since with these variables particles follow circular paths. Note: y' denotes dy/ds while Y' denotes $dY/d\mu$.

The transformation to (Y,Y') is conveniently written in matrix form:

$$\begin{pmatrix} Y \\ Y' \end{pmatrix} = \begin{pmatrix} 1/\sqrt{\beta} & 0 \\ \alpha/\sqrt{\beta} & \sqrt{\beta} \end{pmatrix} \begin{pmatrix} y \\ y' \end{pmatrix}\ . \tag{5.4}$$

Consider now a beam for which the equi-density curves are circles in normalised phase space. If this beam receives an unwanted deflection, D, it will appear at the time of the deflection as shown in Fig. 18(a). However, this asymmetric beam distribution will not persist. As the beam continues along the transfer line, the particles will re-distribute themselves randomly in phase, while maintaining their distance from the origin, so as to restore rotational symmetry. This effect is known as filamentation. Thus after a sufficient time has elapsed the particles, which without the deflection D would have been at point P in Fig. 18(b), will be uniformly distributed at a radius D about the point P.

For one of these particles the projection onto the Y-axis will be

$$Y_2 = Y_1 + D \cos \theta ,$$

where the subscripts 1 and 2 denote the unperturbed and perturbed positions respectively.

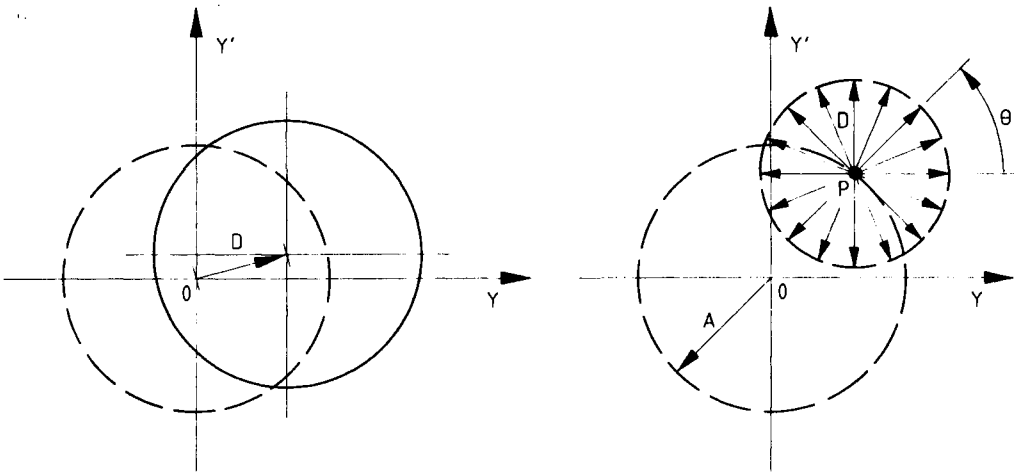

(a) Beam directly after deflection, D

(b) Particle distribution after phase randomisation (Filamentation)

Fig. 18 Effect of an unwanted deflection

Taking the square of this amplitude

$$Y_2^2 = Y_1^2 + 2Y_1 D \cos \theta + D^2 \cos^2 \theta$$

and then averaging over the particles around the point P after filamentation has randomised the kick gives

$$\langle Y_2^2 \rangle_p = \langle Y_1^2 \rangle_p + 2 \langle Y_1 D \cos \theta \rangle_p + \langle D^2 \cos^2 \theta \rangle_p .$$

Since Y_1 and D are uncorrelated (i.e. D does not depend on Y_1), the second term can be written as

$$2 \langle Y_1 \, D \cos \theta \rangle_p = 2 \langle Y_1 \rangle_p \langle D \cos \theta \rangle_p .$$

The second factor is zero, since D is a constant [Fig. 18(a)], which gives

$$\langle Y_2^2 \rangle_p = \langle Y_1^2 \rangle_p + \frac{1}{2} \langle D^2 \rangle_p = \langle Y_1^2 \rangle_p + \frac{1}{2} D^2 \ .$$

However, this result is true for any P at any radius A and hence it is true for the whole beam and

$$\langle Y_2^2 \rangle = \langle Y_1^2 \rangle + \frac{1}{2} D^2 \ . \tag{5.5}$$

The emittance blow-up will be

$$E_2 = E_1 + 2\pi D^2 \ , \tag{5.6}$$

where, by definition, $E = 4\pi \langle Y^2 \rangle$. The subscripts 1 and 2 refer to the unperturbed and perturbed emittances respectively, and remembering that $Y = y/\sqrt{\beta}$.

Expanding the deflection, D,

$$D^2 = (\Delta Y)^2 + (\Delta Y')^2 = (\Delta y)^2 \frac{(1 + \alpha^2)}{\beta} + (\Delta y')^2 \beta \tag{5.7}$$

and substituting into (5.6) gives the emittance blow-up, in terms of the basic errors. Thus

$$E_2 = E_1 + 2\pi \left[(\Delta y)^2 \frac{(1 + \alpha^2)}{\beta} + (\Delta y')^2 \beta \right] \ , \tag{5.8}$$

where

Δy is a beam alignment error,

$\Delta y' = \frac{\ell \Delta B}{B\rho}$ an angle error from a field error ΔB of length ℓ .

5.2 Gradient errors in transfer lines

Consider once again a beam for which the equi-density curves are circles in normalised phase space. If this beam sees a gradient error, k, the equi-density curves directly after the perturbation will be ellipses as shown in Fig. 19(a). Since the object of this analysis is to evaluate the effects of small errors, it is sufficient to regard this gradient error as a thin lens with the transfer matrix

$$\begin{pmatrix} y_2 \\ y_2' \end{pmatrix} = \begin{pmatrix} 1 & 0 \\ k & 1 \end{pmatrix} \begin{pmatrix} y_1 \\ y_1' \end{pmatrix} \ , \tag{5.9}$$

where

$k = \frac{\ell \Delta G}{B\rho}$ an amplitude dependent kick arising from the gradient error ΔG of length ℓ.

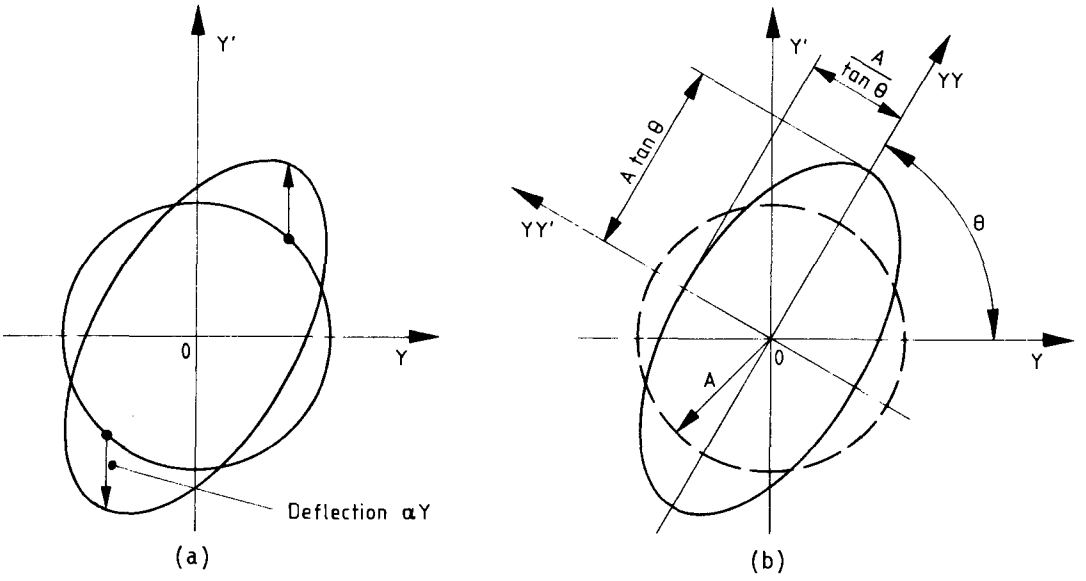

Fig. 19 Effect of a gradient error

Denoting the matrix in Eq. (5.4) as T, it is easy to show that

$$\begin{pmatrix} Y \\ Y' \end{pmatrix}_2 = T \begin{pmatrix} 1 & 0 \\ k & 1 \end{pmatrix} T^{-1} \begin{pmatrix} Y \\ Y' \end{pmatrix}_1 = \begin{pmatrix} 1 & 0 \\ k\beta & 1 \end{pmatrix} \begin{pmatrix} Y \\ Y' \end{pmatrix}_1 .$$

It is now convenient to find a new co-ordinate system (YY,YY'), which is at an angle θ to the (Y,Y') system, and in which the perturbed ellipse is a right ellipse [see Fig. 19(b)].

$$\begin{pmatrix} YY_2 \\ YY' \end{pmatrix}_2 = \begin{pmatrix} c & -s \\ s & c \end{pmatrix} \begin{pmatrix} 1 & 0 \\ k\beta & 1 \end{pmatrix} \begin{pmatrix} Y_1 \\ Y'_1 \end{pmatrix} \tag{5.10}$$

where s and c denote $\sin\theta$ and $\cos\theta$ respectively.

Introducing the initial distribution $Y_1 = A \sin(\mu + B)$, $Y'_1 = A \cos(\mu + B)$, in the above expression for the new distribution, gives

$$\begin{aligned} YY_2 &= A\sqrt{1 + s^2k^2\beta^2 - 2sck\beta}\,\sin(\mu + B + \emptyset) \\ YY'_2 &= A\sqrt{1 + c^2k^2\beta^2 + 2sck\beta}\,\sin(\mu + B + \emptyset') , \end{aligned} \tag{5.11}$$

where

$$\emptyset = \tan^{-1}\left(\frac{-s}{c - sk\beta}\right) \quad \text{and} \quad \emptyset' = \tan^{-1}\left(\frac{c}{s + ck\beta}\right) .$$

The (YY_2, YY_2) ellipse will be a right ellipse when $(\phi-\phi') = \pi/2$, which gives the condition

$$\tan(2\theta) = 2/k\beta \ . \tag{5.12}$$

Equations (5.11) can be simplified using (5.12) and the relationship $(\phi-\phi') = \pi/2$ and rewritten as

$$\begin{pmatrix} YY \\ YY' \end{pmatrix}_2 = \begin{pmatrix} \tan\theta & 0 \\ 0 & 1/\tan\theta \end{pmatrix} \begin{pmatrix} YY \\ YY' \end{pmatrix}_1 \tag{5.13}$$

where

$$\left.\begin{aligned} YY_1 &= A \sin(\mu + B') \\ YY'_1 &= A \cos(\mu + B') \end{aligned}\right\} \text{ i.e. } Y_1 \text{ and } Y'_1 \text{ with a phase shift}$$

$$B' = (B + \phi) = [B + \tan^{-1}(1/\tan\theta)] \ .$$

Thus it has been possible to diagonalise Eq. (5.10) by introducing a phase shift ϕ into the initial distribution. Equation (5.13) is therefore not a true point-to-point transformation, as is Eq. (5.10) but since the initial distribution is rotationally symmetric the introduction of this phase shift has no effect.

The distance from the origin of a perturbed particle is given by Eq. (5.13) as

$$(YY_2^2 + YY'^2_2) = \left[\tan^2\theta\, A^2 \sin^2(\mu + B') + \frac{1}{\tan^2\theta} A^2 \cos^2(\mu + B')\right] .$$

Averaging over 2π in μ gives

$$\langle YY_2^2 + YY'^2_2 \rangle = \frac{1}{2}\left(\tan^2\theta + \frac{1}{\tan^2\theta}\right) \langle A^2 \rangle \ ,$$

but

$$\langle A^2 \rangle = \langle YY_1^2 + YY'^2_1 \rangle = \langle Y_1^2 + Y'^2_1 \rangle$$

and from (5.12)

$$\left(\tan^2\theta + \frac{1}{\tan^2\theta}\right) = k^2\beta^2 + 2 \ .$$

Thus,

$$\langle YY_2^2 + YY'^2_2 \rangle = \frac{1}{2}(k^2\beta^2 + 2) \langle YY_1^2 + YY'^2_1 \rangle \ . \tag{5.14}$$

As in the previous case for dipole errors, the asymmetric beam distribution will not persist. The beam will regain its rotational symmetry by filamentation or phase randomisation. Each particle, however, will maintain constant its distance from the origin. Once filamentation has occurred, the distribution will not distinguish between the YY and YY' axes and Eq. (5.14) can be rewritten as

$$\langle YY_2^2 \rangle = \frac{1}{2} (k^2\beta^2 + 2) \langle YY_1^2 \rangle \tag{5.15}$$

and hence the emittance blow-up will be

$$E_2 = \frac{1}{2} (k^2\beta^2 + 2) E_1 \ . \tag{5.16}$$

For a series of errors the order must be respected and complete randomisation is assumed between them. This is clearly not true in a real-world situation but this analysis does give an approach for specifying power supply tolerances for example.

5.3 Dipole errors in circular machines

In Section 3.4 the equation of motion was derived for a momentum error, this is analogous to a momentum error which is a function of the position round the machine. By directly translating $\Delta p/p$ into $\Delta B/B$ we get

$$\frac{d^2y}{ds^2} + K(s)y = (\text{sign}) \frac{\Delta B(s)}{B\rho} \quad , \tag{5.17}$$

where (sign) = -1 when the field error is in the plane of bending and +1 when it is perpendicular to the plane of bending.

The betatron oscillation of Eq. (4.4) executes Q * oscillations when going round a circular machine. Q is known as the tune of the machine. It is useful to use this fact to normalise the betatron phase advance, μ, into a variable, $\emptyset$, which changes from 0 to 2π in a single turn. If the displacement, y, is divided by $\sqrt{\beta}$, we have what are known as the normalised variables (Y, $\emptyset$). Equation (5.17) can be re-expressed, using these variables, to give

$$\frac{d^2Y}{d\emptyset^2} + Q^2Y = -Q^2\beta^{3/2} (\text{sign}) \frac{\Delta B}{B\rho} \ . \tag{5.18}$$

This form of the equation allows us to use all the known results for driven harmonic oscillators, but first consider only a single kick ΔB at $s = s_0$. The solution to the inhomogeneous Eq. (5.18) is then a betatron oscillation launched at $s = s_0$ with an angle $(\Delta B\ \Delta s)/B\rho$. If we add to this, a solution to the homogeneous equation such that the sum of the two solutions returns the input conditions, we get the situation in Fig. 20, where the addition of the two oscillations, which are not individually closed round the machine, make a continuous trajectory, called the closed orbit. If there are many field errors the individual solutions can be added linearly. The formal expression for the closed orbit is given below.

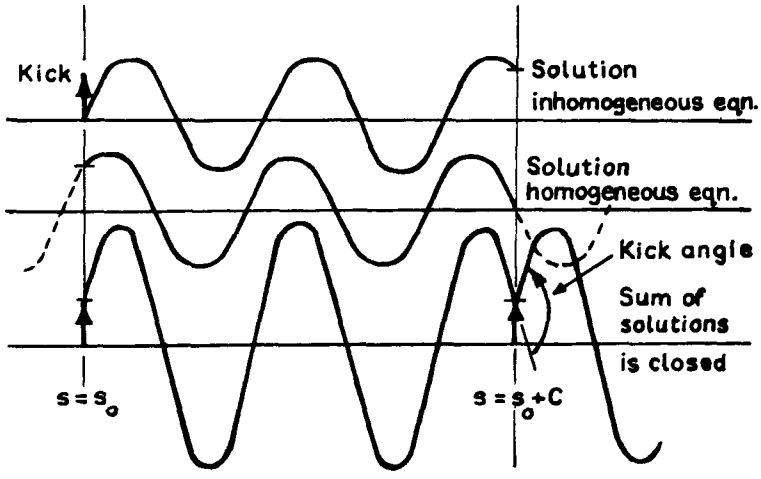

Fig. 20 Effect of a single field error

$$Y(\emptyset) = (\text{sign}) \frac{Q}{2 \sin \pi Q} \int_{\emptyset}^{\emptyset+2\pi} \beta^{3/2} \frac{\Delta B}{B\rho} (\psi) \cos Q (\pi + \emptyset - \psi) \, d\psi \, , \qquad (5.19)$$

where ψ is a variable in $\emptyset$ used for the integration only.

Certain features of interest can be seen in Eq. (5.19). Firstly if Q is integer, then $Y(\emptyset)$ goes to infinity, since $\sin \pi Q = 0$. The integer number of oscillations causes the error to reinforce its effect on each turn. At a point 180° in $\emptyset$ round the machine from a single error, Y must be a maximum or a minimum. At the error the orbit displacement is

$$y = \frac{1}{2} (\text{sign}) \beta \frac{\Delta B \ell}{B\rho} \cot (\pi Q) \, .$$

Also by suitably manipulating (5.19) the conditions for local bumps can be found.

5.4 Gradient errors in circular machines

Suppose we introduce a gradient error of focal length F into an accelerator at one point. The transfer matrix for one turn then becomes

$$M = \begin{pmatrix} \cos \mu + \alpha \sin \mu & \beta \sin \mu \\ -\gamma \sin \mu & \cos \mu - \alpha \sin \mu \end{pmatrix} \begin{pmatrix} 1 & 0 \\ -\frac{1}{F} & 1 \end{pmatrix}$$

$$M = \begin{pmatrix} \cos \mu + \alpha \sin \mu - \frac{\beta}{F} \sin \mu & \beta \sin \mu \\ -\gamma \sin \mu - \frac{1}{F} (\cos \mu - \alpha \sin \mu) & \cos \mu - \alpha \sin \mu \end{pmatrix}$$

Thus the average field must increase at twice the rate of the guiding field, which is known as the "2-to-1" rule. This device has the advantage of being simple, but it is limited in energy by saturation in the iron core and the size of the magnet required. The energy transferred to the beam comes from the stored magnetic energy and is proportional to the flux change.

7.2 Accelerating cavities

Let us consider first a resonant lumped circuit of a parallel plate capacitor bridged by an inductance (see Fig. 22). If we wish to raise the frequency of this circuit we have to reduce C, by separating the plates, and reduce L, by removing turns from the inductance. Gradually the inductance becomes a straight wire and then forms the walls of a box or cavity.

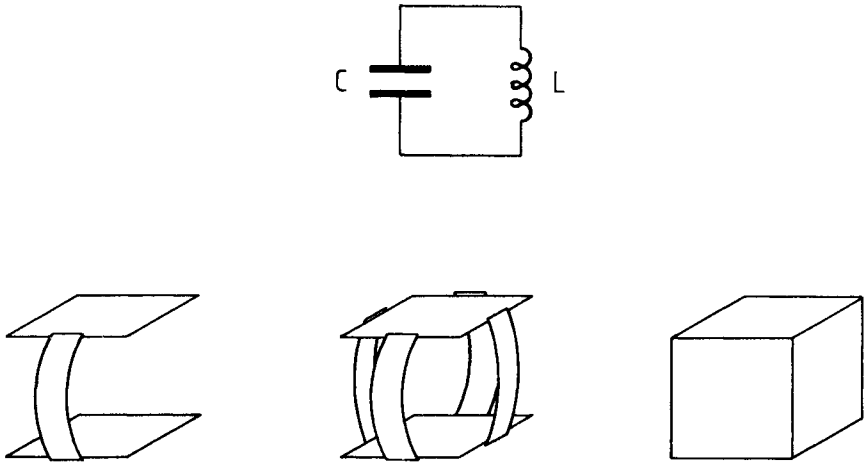

Fig. 22 Evolution from a lumped circuit to a cavity

In this way, one can build a resonant circuit (cavity), which can work at the high frequencies seen in accelerators.

A less descriptive approach to cavities is to first consider free space electromagnetic waves:

$$\left.\begin{aligned} \underline{\nabla} \times \underline{E} &= -\mu \frac{\partial \underline{H}}{\partial t} \\ \underline{\nabla} \times \underline{H} &= \varepsilon \frac{\partial \underline{E}}{\partial t} \end{aligned}\right\} \rightarrow \left\{\begin{aligned} \nabla^2 \underline{E} &= \mu\varepsilon \frac{\partial^2 \underline{E}}{\partial t^2} \\ \nabla^2 \underline{H} &= \mu\varepsilon \frac{\partial^2 \underline{H}}{\partial t^2} \end{aligned}\right.$$

where μ and ε are the permeability and dielectric constant of free space respectively.

When solving these equations the boundary conditions lead to different types of solutions, which can be generally classified as:

TEM waves	No $\underline{E}$ or $\underline{H}$ component in direction of propagation. $\underline{E}$ and $\underline{H}$ transverse only.
H-waves or TE waves	$\underline{H}$ in direction of propagation. $\underline{E}$ transverse to direction of propagation.

E-waves or TM waves E in direction of propagation. H transverse to direction of propagation.

Waves guided by conducting plates in three different geometries are of special interest to us, (i) radial transmission line, (ii) cylindrical wave guide, and (iii) co-axial line. These cases are sketched below.

(i) Radial transmission line

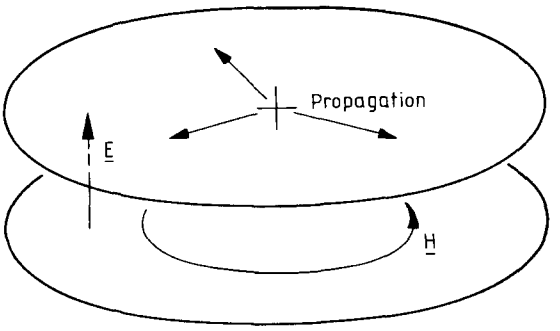

(ii) Cylindrical waveguide

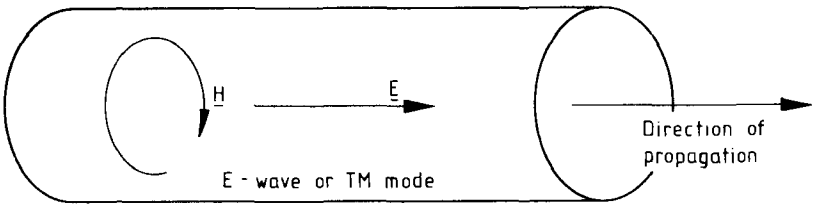

(iii) Co-axial line

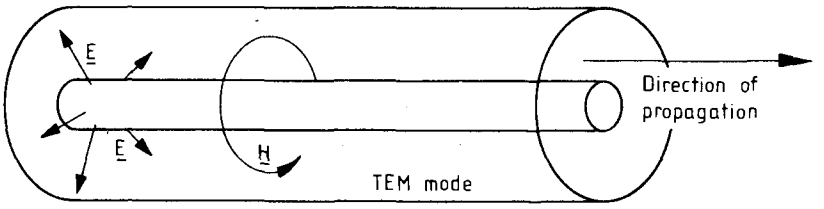

Cavities are formed by shorting any of these guiding systems either by conducting walls where E → 0 or by a capacitive gap where E → maximum, so that standing waves can be excited in resonance. There are basically two types of cavity of interest to us.

7.2.1 Radial line resonator

Figure 23 shows the basic mode for fields inside a "pill-box" cavity. This mode can either be regarded as a shorted radial transmission line (i.e. 2 parallel discs guiding waves radiating from the centre) with a standing wave mode or as a cylindrical waveguide mode at cut-off. In the first case, it is called a radial line resonator and in the second a TM_{010} resonator. TM indicates that the magnetic field is transverse to the s-axis along which the electric field is aligned and that this axis would be the direction of propagation in the waveguide. The suffixes indicate the number of waves in the field first azimuthally, then radially and finally axially (note: not the normal co-ordinate order).

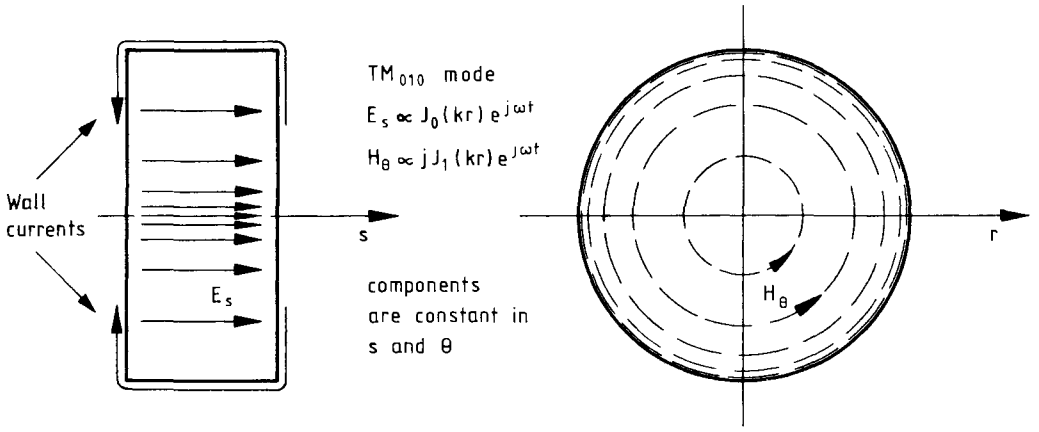

Fig. 23 Pill-box cavity or radial line resonator with the TM_{010} mode

If we make a small hole on the s-axis and send an ion through at the correct moment in time, it will see the maximum axial electric field,

$$E_s \propto J_0(kr)\, e^{j\omega t}$$

$$B_\theta \propto jJ_1(kr)\, e^{j\omega t}\ , \tag{7.8}$$

where

k is a constant depending on geometry

J_0 and J_1 are Bessel Functions.

The magnetic field, B_θ, is 90° out of phase with E_s and thus when E_s is maximum, the rate of change of the magnetic field, $\partial B_\theta/\partial t$ is also a maximum. The accelerating voltage is induced by the varying field just as in the betatron only the topology is inverted; instead of the beam surrounding the field, the field surrounds the beam (see Fig. 24). In this way energy can be taken out of the field on each passage, which would not be possible in an electrostatic field. The sinusoidal time variation in the field is therefore needed, but as we shall see later it also provides an important mechanism for focusing.

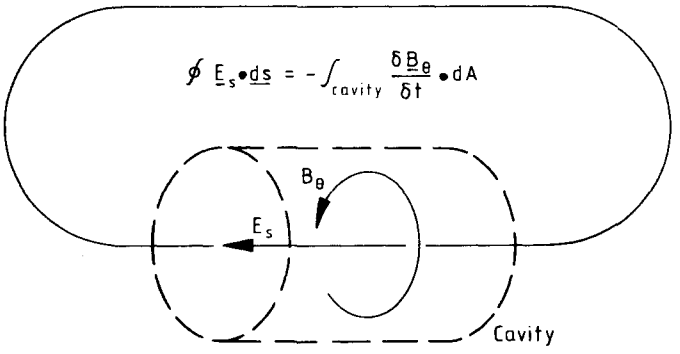

Fig. 24 Action of a cavity

7.2.2 Foreshortened co-axial and radial line resonators

By starting with two co-axial plates as the capacitor in Fig. 22 it would be logical to end up with a shorted co-axial line resonator. In this resonator the electric field vector is radial, which is of no use to us, but by opening a gap as shown in Fig. 25, there is an axial field again, and the resonator is termed foreshortened. The resonant length is a quarter wavelength and the maximum electric field appears across the gap.

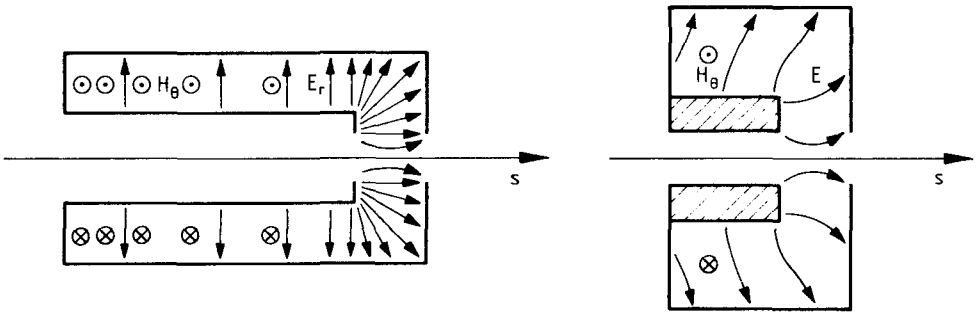

Fig. 25 Foreshortened co-axial and radial line resonators

If the dimensions are larger radially than axially, the resonator is called a foreshortened radial line resonator, which brings us back to the first cavity. In practice, the shape can be distorted in many ways, the volume loaded with ferrite and so on.

7.3 Phase stability

When an ion passes through the accelerating cavity it sees an electric field and receives a step, δE, in its energy equal to its charge times the cavity voltage at that moment.

$$\delta E = eV \sin \phi \tag{7.9}$$

where

V is the maximum cavity voltage

ϕ is the phase of the cavity voltage as the ion traverses the cavity.

Ideally we now increase the field in the machine, so that the particle continues round the machine on the same orbit as before. We also adjust the frequency of the cavity such that when the particle re-enters the cavity one turn later the cavity voltage has the same phase. This ideal particle is called the synchronous particle and the phase of the cavity voltage is called the synchronous phase, ϕ_S. The above is easily said and less easily achieved. The energy gain appears as a velocity gain, which determines the necessary increase in frequency, and also as a mass gain, which with the velocity determines the increase necessary in the strength of the guide field. Since magnets have non-linear excitation curves, there is one more factor to include. Satisfying the requirements of

the synchronous particle is analagous to designing the central orbit, but just as focusing was needed to keep the beam close to the central orbit, so we will also need focusing to keep the natural energy spread of the beam clustered around the energy of the synchronous particle.

Consider now some particles which have small energy deviations from the synchronous particle. Because they have different energies their speeds are different and their momenta are different. The speed directly affects the revolution period and the momentum indirectly affects the revolution period since the particle will follow a new orbit of a different length. We must next discover whether an increase in energy also means an increase in revolution frequency due to the speed increase, or a decrease in revolution frequency due to the relativistic momentum increase, which requires more field to achieve 2π radians of bending and hence a longer orbit.

To do this we express the revolution time, τ, as a function of orbit length and speed,

$$\tau = \frac{C}{v} \quad ,$$

giving

$$\frac{d\tau}{\tau} = \left(\frac{dC}{C} - \frac{dv}{v}\right) = \left(\frac{dR}{R} - \frac{dv}{v}\right) \quad , \tag{7.10}$$

where C = machine circumference = $2\pi R$ and R is the average machine radius.

Firstly we define the momentum compaction factor, α, as

$$\alpha = \Delta R \Big/ \frac{\Delta p}{p} \quad , \tag{7.11}$$

which is a measure of the proximity of the orbits of different momenta. This factor depends on the machine optics and is determined by averaging the dispersion function, D(s) of Eq. (3.23) so that $\alpha = \overline{D}$. This is a source of some possible confusion, since α is sometimes defined as

$$\alpha = \frac{\Delta R}{R} \Big/ \frac{\Delta p}{p}$$

and the dispersion function D is often denoted by α_p.

The term dv/v (or $d\beta/\beta$ where $\beta = v/c$) can be re-expressed as

$$\frac{dv}{v} = \frac{1}{\gamma^2} \frac{dp}{p} \quad , \tag{7.12}$$

where

$$\gamma = \frac{E}{E_0} = \frac{M}{M_0} \text{ the energy in units of the rest energy.}$$

Here we have used β and γ in their traditional roles in relativity theory and hopefully there will be no confusion with the earlier use as Courant and Snyder parameters.

Substituting Eqs. (7.11) and (7.12) in (7.10) we have

$$\frac{d\tau}{\tau} = -\frac{df}{f} = \frac{\Delta p}{p}\left(\frac{\alpha}{R} - \frac{1}{\gamma^2}\right) . \tag{7.13}$$

Clearly $d\tau$ changes sign as $1/\gamma^2$ becomes larger than α/R and this transition occurs at what is known as the transition energy, γ_t,

$$\gamma_t^2 = R/\alpha . \tag{7.14}$$

Finally we express Eq. (7.13) in the form

$$\eta = \left(\frac{\Delta f}{f} \Big/ \frac{\Delta p}{p}\right) = \left(\frac{1}{\gamma^2} - \frac{1}{\gamma_t^2}\right) . \tag{7.15}$$

Thus the revolution frequency increases with $\Delta p/p$ while the machine is working below the transition energy, but this situation is reversed as soon as $\gamma > \gamma_t$. The frequency spread with unit momentum spread is traditionally represented by η and is sometimes defined with the opposite sign.

Assuming first that the accelerator is working below transition, we follow a particle which is slightly more energetic than the synchronous particle. By Eq. (7.15) we see that this particle will arrive at the cavity a little ahead of the synchronous particle, since its revolution frequency is higher. If we arrange the cavity voltage as shown in Fig. 26 the voltage seen by this particle will be lower, the energy gain will be lower than that of the synchronous particle and consequently on the next turn the particle will slip back towards the synchronous particle. Conversely, if the particle has a lower energy, it turns more slowly in the machine, but by the time it reaches the cavity the voltage has had time to rise higher, which means the particle gets a bigger kick to help it catch up the synchronous particle. Within limits the cavity voltage can be considered linear and the energy given to the particle varies linearly with the lag or lead with respect to the synchronous particle. The second diagram in Fig. 26 shows the inverted situation when the accelerator is working above transition. Over many turns, the off-momentum particles will lead and lag and lead and so on, the synchronous particle. The resultant oscillations are known as synchrotron oscillations (see Fig. 27). In this way the voltage ramp has a focusing action.

A more quantitive approach is as follows.

The energy increment received by the synchronous particle is merely that of Eq. (7.9) with the appropriate synchronous phase. This increment will be the difference in energy between the kth and (k-1)th turns, which for the synchronous particle we fix as constant for all k,

$$\delta E_s = (E_{k,s} - E_{k-1,s}) = eV \sin \phi_s \tag{7.16}$$

and likewise for a general particle

$$\delta E = (E_k - E_{k-1}) = eV \sin \phi . \tag{7.17}$$

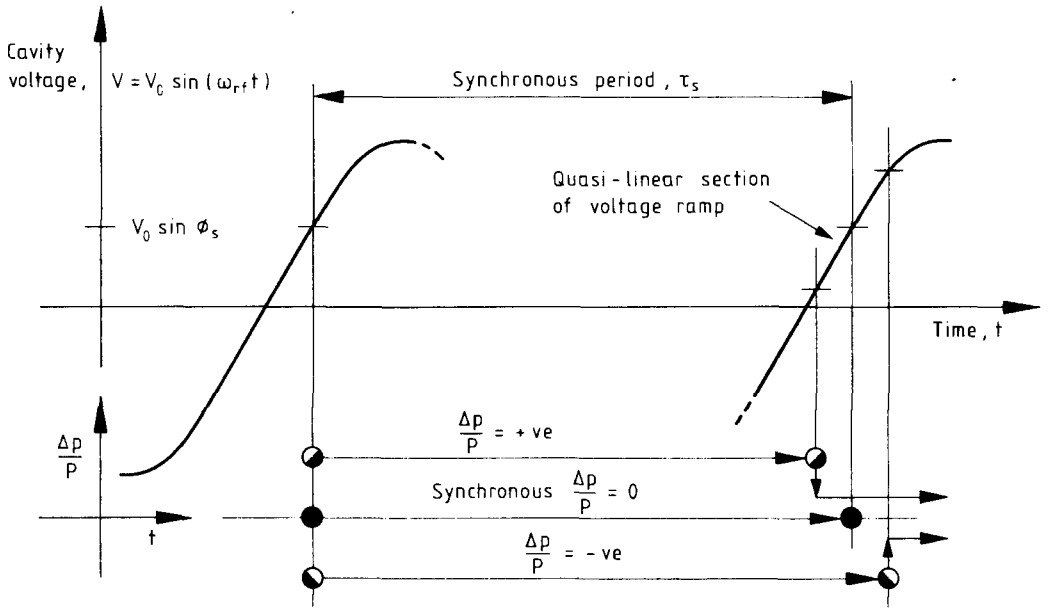

(i) Operation below transition

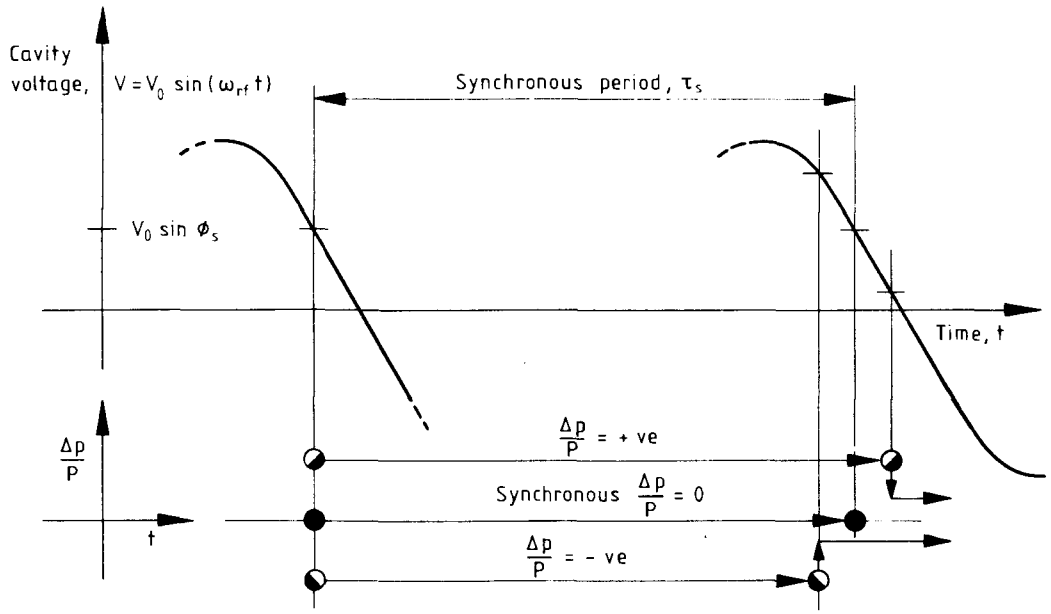

(ii) Operation above transition

Fig. 26 Focusing action of the accelerating voltage

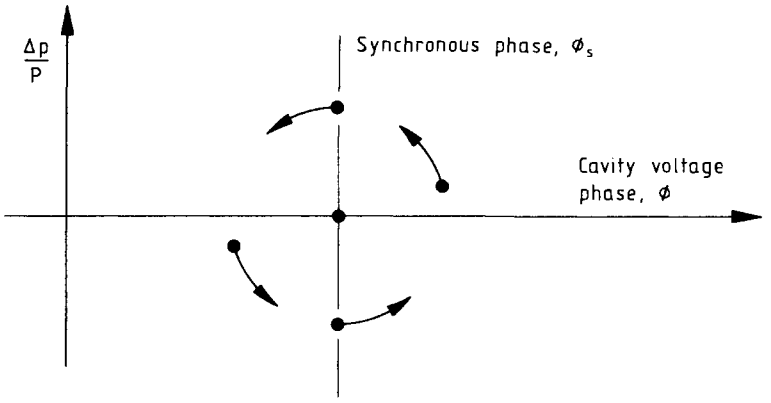

Fig. 27 Synchrotron oscillations

Just as we described orbits with respect to the central orbit, we now wish to describe the energy oscillations of the non-synchronous particles with respect to the synchronous particle. Defining the energy difference with the synchronous particle as $\Delta E_k = (E_k - E_{k,s})$, we have

$$(E_k - E_{k,s}) - (E_{k-1} - E_{k-1,s}) = eV (\sin \phi - \sin \phi_s)$$

$$(\Delta E_k - \Delta E_{k-1}) = eV (\sin \phi - \sin \phi_s) \ . \tag{7.18}$$

Assuming that ϕ and E change slowly, which is generally the case, we convert the difference Eq. (7.18) into a differential equation. If there are n accelerations per second, then $dn/dt = \omega_{rev}/2\pi$ for a single cavity, where ω_{rev} is the revolution frequency for the synchronous* particle,

$$\frac{1}{\omega_{rev}} \frac{d\Delta E}{dt} = \frac{eV}{2\pi} (\sin \phi - \sin \phi_s) \ . \tag{7.19}$$

Returning to the synchronous particle, we know that in order for synchronisation to be maintained

$$\omega_{rf} = h \, \omega_{rev} \ , \tag{7.20}$$

where

ω_{rf} is the cavity frequency

h is known as the harmonic number and is of course integer.

Now the rate of phase slip of the general particle is $d\phi/dt$ and the phase slip in one turn will be $\tau_{rev} \, d\phi/dt$. Alternatively, we can express this as the excess time needed to make one turn, $\Delta\tau$, multiplied by ω_{rf} from Eq. (7.20). Thus,

---

* The subscript "s" is used to denote the synchronous particle, but for the revolution frequency it is customary to put ω_{rev} to avoid a possible confusion with the synchrotron frequency.

$$\tau_{rev} \frac{d\phi}{dt} = \Delta\tau \; h\omega_{rev} \; . \tag{7.21}$$

Here we speak loosely about the phase of the particle meaning the phase of the cavity when the particle arrives.

We have already got an expression for $\Delta\tau$ in Eq. (7.13). So we can write

$$\frac{d\phi}{dt} = h\omega_{rev} \frac{\Delta p}{p} \left(\frac{1}{\gamma_t^2} - \frac{1}{\gamma_s^2}\right) \; ,$$

but $\Delta p/p$ can be written as $\Delta E/\beta_s^2 E_s$ giving

$$\frac{d\phi}{dt} = h\omega_{rev} \; \Gamma \frac{\Delta E}{E_s} \; , \tag{7.22}$$

where

$$\Gamma = \frac{1}{\beta_s^2} \left(\frac{1}{\gamma_t^2} - \frac{1}{\gamma_s^2}\right) \; .$$

Combining Eqs. (7.19) and (7.22), we find

$$\frac{1}{\omega_{rev}} \frac{d}{dt} \left(\frac{E_s}{h\omega_{rev}\Gamma} \frac{d}{dt} \phi\right) = \frac{eV}{2\pi} (\sin\phi - \sin\phi_s),$$

going to

$$\frac{E_s}{\omega_{rev}^2 h\Gamma} \frac{d^2\phi}{dt^2} = \frac{eV}{2\pi} (\sin\phi - \sin\phi_s) \tag{7.23}$$

if we assume ω_{rev} and Γ vary slowly - <u>adiabatic limit</u>.

Suppose the oscillations are small and the general particle sees only small changes in the cavity phase,

$$\phi = \phi_s + \delta\phi \quad \text{where} \quad \delta\phi \ll 1 \; ,$$

then the right-hand side of Eq. (7.23) becomes

$$\frac{eV}{2\pi} (\sin\phi_s \cos\delta\phi + \sin\delta\phi \cos\phi_s - \sin\phi_s)$$

$$= \frac{eV}{2\pi} \delta\phi \cos\phi_s$$

Since ϕ_S = constant, Eq. (7.23) becomes

$$\frac{d^2}{dt^2}(\delta\phi) + \left[-\frac{eV\omega_{rev}^2 h\Gamma\cos\phi_s}{2\pi E_s}\right]\delta\phi = 0 \qquad (7.24)$$

$$\frac{d^2}{dt^2}\delta\phi + \Omega^2\delta\phi = 0 \ . \qquad (7.25)$$

where Ω is called the synchrotron frequency.

Equation (7.25) can be stable or unstable depending on (cos ϕ_S Γ).

(a) Stable oscillations if, Γ cos $\phi_S < 0$, sin ϕ close to sin ϕ_S.

(b) Unstable oscillations if, Γ cos $\phi_S > 0$. (Unstable equilibrium for synchronous particle.)

This is another way of saying that the correct slope for the voltage ramp must be chosen in Fig. 26. The incorrect slope quickly drives the particle further from synchronism.

If the oscillation is stable the particle is said to be trapped by the rf.

Clearly the ramp is only linear over a limited region in ϕ or $\Delta\tau$ the lag or lead of the particle with respect to the synchronous particle. Particles far from the linear region are not trapped but only disturbed by the rf forces. The area in the $(\Delta p/p,\phi)$ space which is stable or in which particles can be trapped is called a <u>bucket</u>.

If the harmonic number is large then the voltage ramp is steep, the stable region narrow and the focusing forces strong. The small buckets will then contain short bunches.

If sin ϕ_S is increased the energy per turn increases and acceleration is quicker, but the linear region on the ramp is restricted.

Finally if sin ϕ_S = 0, there is no net acceleration, but particles are still trapped and the linear region on the ramp is maximum.

Returning to Eq. (7.23), we have

$$\frac{E_s}{h\omega_{rev}^2 h\Gamma}\frac{d^2\phi}{dt^2} - \frac{eV}{2\pi}\sin\phi = -\frac{eV}{2\pi}\sin\phi_s \ .$$

This is <u>similar</u> to the equation for a biased pendulum (see Fig. 28).

In both positions the moment of the pendulum balances the counterweight. In position (a) it is stable since small displacements will cause the pendulum to oscillate. In position (b) the slightest force will unbalance the system. The first position is the stable fixed point and the second the unstable fixed point.

Most AG accelerators span the energy range 1 to 20 times the injection energy. This usually crosses the transition energy, so that we have the problem of jumping transition, i.e. crossing from Fig. 26 (i) to 26 (ii).

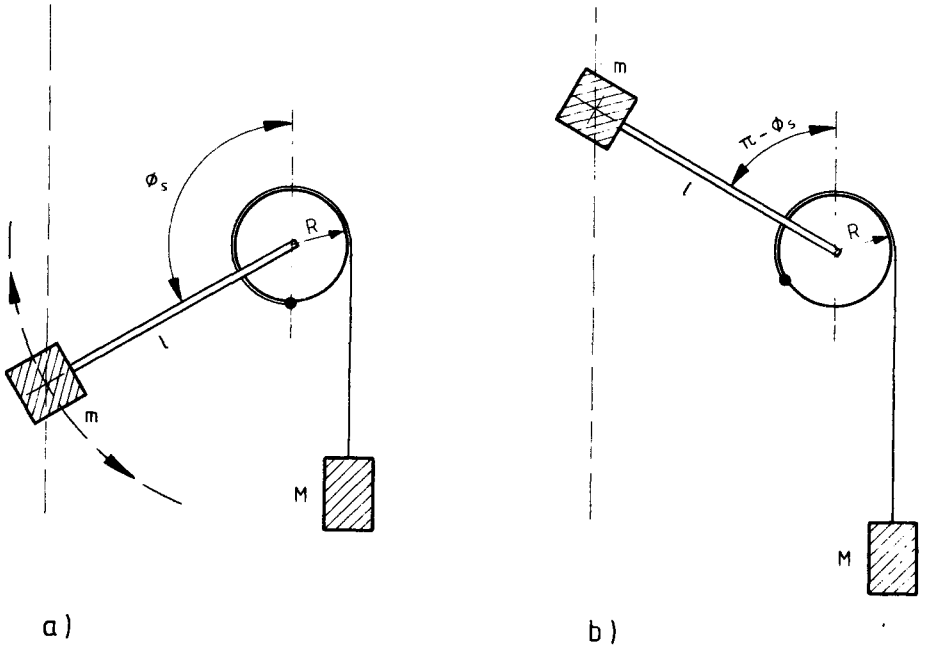

Fig. 28 Biased pendulum

Equation (7.15) tells us that as we approach the transition energy the frequency spread for unit momentum spread, η, goes to zero. This causes the particles to be bunched tightly in terms of phase but the bunches will have a large Δp. The slow synchrotron frequency and the tight bunching in phase make it possible to jump from Fig. 26 (i) to 26 (ii) and re-trap the beam.

BIBLIOGRAPHY

M.H. Blewett (ed.), Theoretical aspects of the behaviour of beams in accelerators and storage rings, Proceedings of the First Course of the International School of Particle Accelerators of the "Ettore Majorana" Centre for Scientific Culture, Erice, 10-22 November 1976, CERN 77-13.

C. Bovet et al., A selection of formulae and data useful for the design of AG synchrotrons, CERN/MPS-SI/Int. DL/70/4.

P. Brummer, The Method of measurement of the emittance and the betatron phase space parameters in the beam transfer system of the ISR, ISR-OP/72-6, (1972).

R.A. Carrigan, F.R. Huson and M. Month (eds.), Physics of high energy particle accelerators, Fermilab Summer School 1981, American Institute of Physics Conference Proceedings No. 87, 1982.

E.D. Courant and H.S. Snyder, Theory of the alternating-gradient synchrotron, Ann. Phys. 3, 1-48, 1958.

E. Fischer, Beam blow-up due to multiple scattering in the injection windows, ISR-VA/EF/sm (1974).

G. Guignard, Selection of formulae concerning proton storage rings, CERN 77-10 (1977).

H.G. Hereward, How good is the r.m.s. as a measure of beam size? CERN/MPS/DL 69-15 (1969).

J.J. Livingood, Principles of cyclic particle accelerators, (D. Van Nostrand Company Inc. 1961).

Particle Data Group, Review of particle properties, CERN, Geneva, August 1982 (reprinted from Physics Letters, vol. 111B, April 1982).

E. Persico, E. Ferrari and S. Segrè, Principles of particle accelerators (W.A. Benjamin, New York, 1968).

S. Ramo and J. Whinnery, Fields and Waves in Modern Radio, (J. Wiley, New York, 1962), 2nd edn.

C. Wyss, A measuring system for magnets with cylindrical symmetry", in Proceedings of the 5th International Conference on Magnet Technology, Rome, 1975 (Laboratori Nazionali del CNEN, Frascati, 1975), p. 231.

This final expression is well known in the accelerator field for protons as

$$B_z\rho_0 = 3.3356\ p \qquad (A8)$$

where

$(B_z\rho_0)$ is known as the magnetic rigidity in units of [Tm] remembering that B_z is the field component perpendicular to the motion,

p is the momentum in units of [GeV/c],

the constant = $10^9/c = 3.3356$.

One can, of course, arrive very quickly at the final result if one cheats slightly and assumes the circular trajectory for reasons of symmetry and invokes the useful engineering notion of centrifugal force. One then considers the rotating particle as being in equilibrium between this force and the magnetic force (see Fig. A2).

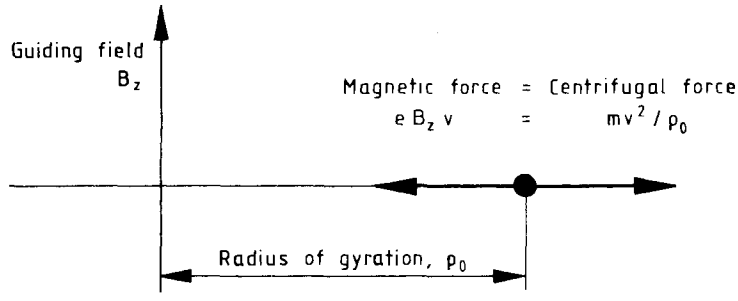

Fig. A2 Balance of forces in cyclotron motion

Finally in Eq. (A3) v_z was found to be constant and tacitly assumed to be zero. Of course, v_z need not be zero and in a uniform field as described, it would remain constant and stretch the cyclotron motion into a spiral. Without focusing, therefore, the smallest vertical angle error in a cyclotron would cause the beam to spiral up or down and hit the poles.

APPENDIX B

TRACKING THROUGH 3-DIMENSIONAL FIELD PLOTS

In Appendix A, it was shown that in a uniform magnetic field an ion with velocity $\underline{v}$ would move on a circular orbit transversely to the magnetic field and on a straight line parallel to the field. The combination of these motions being a spiral in the field direction. By assuming that over very small volumes of space the field $\underline{B}$ is constant, this simple result can be used to track through complicated field plots. The accuracy then depends upon how fine a mesh is used for the tracking, on the accuracy of interpolation between the mesh points in the field plot and on the accuracy of the plot itself.

Consider a particle of momentum $\underline{p}$ at the origin of the (x,y,z) frame which is aligned with the field plot. We then choose a second frame (xx,yy,zz) with the same origin which is aligned with the field $\underline{B}$ and force $\underline{F}$ remembering that the force is mutually perpendicular to $\underline{B}$ and $\underline{p}$ (i.e. $m\underline{v}$).

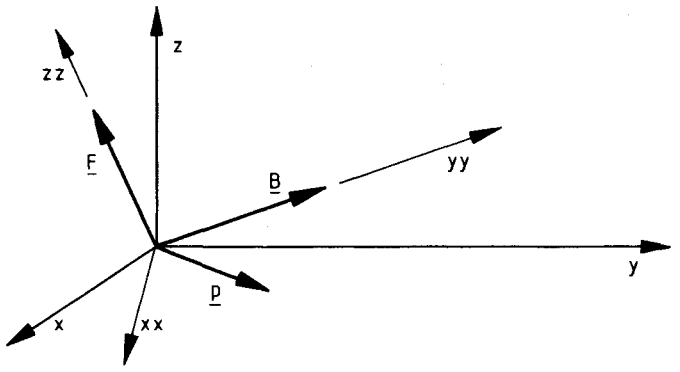

Now,

$$\underline{p} = p_x\underline{i} + p_y\underline{j} + p_z\underline{k} \quad \text{and put} \quad |\underline{p}| = p$$

$$\underline{B} = B_x\underline{i} + B_y\underline{j} + B_z\underline{k} \quad \text{and put} \quad |\underline{B}| = B \ .$$

Let values at the origin be suffixed by 0.

The momentum can be resolved into two components - p_L parallel to $\underline{B}$ and p_T transverse to $\underline{B}$, i.e.

$$p_L = \frac{1}{B} \ (\underline{p}\cdot\underline{B}) = \frac{(B_x p_x + B_y p_y + B_z p_z)}{(B_x^2 + B_y^2 + B_z^2)^{1/2}}$$

$$p_T = \sqrt{p^2 - p_L^2}$$

$$\rho = \frac{3.3356}{B} \, p_T \qquad \text{Eq. (A8) Appendix A.}$$

The motion parallel to $\underline{B}$ is unaffected while the motion transverse to $\underline{B}$ is made into a cyclotron motion. Looking in the frame (xx,yy,zz) we see

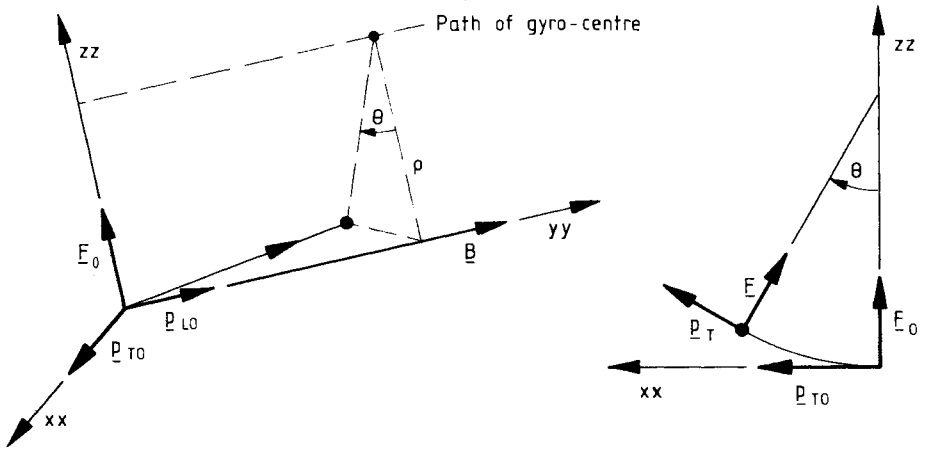

Since the 'yy' motion is uniform we can simply look at the xx-zz plane.

Let us specify that the field $\underline{B}$ is acceptably constant over a distance ℓ, then the new positions are

$$xx = \rho \sin \theta = \rho \sin \left(\frac{p_{TO}}{p}\frac{\ell}{\rho}\right)$$

$$zz = \rho(1 - \cos \theta) = \rho\left[1 - \cos \left(\frac{p_{TO}}{p}\frac{\ell}{\rho}\right)\right]$$

$$yy = \frac{p_L}{p}\ell$$

and momentum components are

$$p_{xx} = p_{TO} \cos \left(\frac{p_{TO}}{p}\frac{\ell}{\rho}\right)$$

$$p_{zz} = p_{TO} \sin \left(\frac{p_{TO}}{p}\frac{\ell}{\rho}\right)$$

$$p_{yy} = p_{LO} \cdot$$

It remains to transfer the new (xx,yy,zz) values for position and momentum into the (x,y,z) frame.

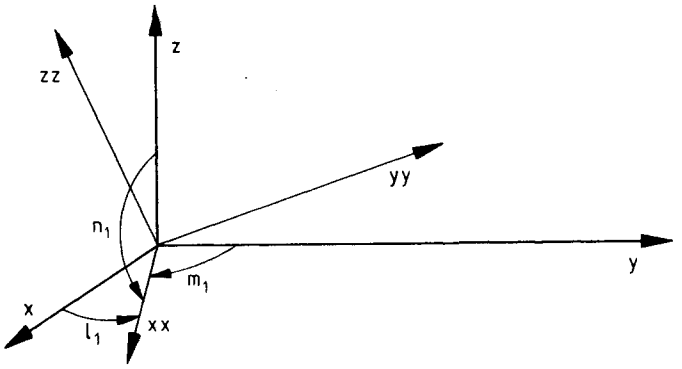

Let the direction cosines of 'xx' in the (x,y,z) frame be

$$(\ell_1, m_1, n_1) \ .$$

Similarly, for, 'yy' (ℓ_2, m_2, n_2)

and, 'zz' (ℓ_3, m_3, n_3) .

To transform (xx,yy,zz) we then have

$$\begin{pmatrix} x \\ y \\ z \end{pmatrix} = \begin{pmatrix} \ell_1 & \ell_2 & \ell_3 \\ m_1 & m_2 & m_3 \\ n_1 & n_2 & n_3 \end{pmatrix} \begin{pmatrix} xx \\ yy \\ zz \end{pmatrix}$$

or

$$\begin{pmatrix} p_x \\ p_y \\ p_z \end{pmatrix} = \begin{pmatrix} \ell_1 & \ell_2 & \ell_3 \\ m_1 & m_2 & m_3 \\ n_1 & n_2 & n_3 \end{pmatrix} \begin{pmatrix} p_{xx} \\ p_{yy} \\ p_{zz} \end{pmatrix}$$

Since 'yy is coincident with $\underline{B}$ they have the same direction cosines, i.e.

$$\ell_2 = \frac{B_{x0}}{B} , \quad m_2 = \frac{B_{y0}}{B} , \quad n_2 = \frac{B_{z0}}{B} .$$

Now 'zz' is coincident with $\underline{F}$, i.e. $(\underline{p} \times \underline{B})e/m$. The unit $\underline{F}$ vector is therefore $(\underline{p} \times \underline{B})/pB \sin\theta$ where $\sin\theta = p_{T0}/p$, hence,

$$\ell_3 = \frac{1}{pB} (B_{z0}p_{y0} - B_{y0}p_{z0}) \frac{1}{\sin\theta}$$

$$m_3 = \frac{1}{pB} (B_{x0}p_{z0} - B_{z0}p_{x0}) \frac{1}{\sin\theta}$$

$$n_3 = \frac{1}{pB} (B_{y0}p_{x0} - B_{x0}p_{y0}) \frac{1}{\sin\theta} \ .$$

Finally 'xx' is mutually perpendicular to 'yy' and 'zz' in a right-handed system so that the unit vector $\underline{i}_{xx} = \underline{j}_{yy} \times \underline{k}_{yy}$ giving

$$\ell_1 = m_2 n_3 - m_3 n_2$$

$$m_1 = \ell_3 n_2 - \ell_2 n_3$$

$$n_1 = \ell_2 m_3 - m_2 \ell_3 \ .$$

Thus,

$$x = x_0 + xx\ell_1 + yy\ell_2 + zz\ell_3$$
$$y = y_0 + xxm_1 + yym_2 + zzm_3$$
$$z = z_0 + xxn_1 + yyn_2 + zzn_3 \ .$$

Such calculations are impossibly complicated by hand, but superbly adapted to a computer. It only remains to check if the field at the end point of a step is within a certain tolerance equal to the field at the start. If not, ℓ must be reduced, if yes, the initial and end fields can be averaged and the step recalculated, and so on.